REPORT 1057

ANALYSIS OF THE EFFECTS OF BOUNDARY-LAYER CONTROL ON THE TAKE-OFF AND POWER-OFF LANDING PERFORMANCE CHARACTERISTICS OF A LIAISON TYPE OF AIRPLANE [1]

By Elmer A. Horton, Laurence K. Loftin, Jr., Stanley F. Racisz, and John H. Quinn, Jr.

SUMMARY

A performance analysis has been made to determine whether boundary-layer control by suction might reduce the minimum take-off and landing distances of a four-place or five-place airplane or a liaison type of airplane below those obtainable with conventional high-lift devices. The airplane was assumed to have a cruise duration of 5 hours at 60-percent power and to be operating from airstrips having a ground friction coefficient of 0.2 or a combined ground and braking coefficient of 0.4. The pay load was fixed at 1500 pounds, the wing span was varied from 25 to 100 feet, the aspect ratio was varied from 5 to 15, and the power was varied from 300 to 1300 horsepower. Maximum lift coefficients of 5.0 and 2.8 were assumed for the airplanes with and without boundary-layer control, respectively. A conservative estimate of the boundary-layer-control-equipment weight was included. The effects of the boundary-layer control on total take-off distance, total power-off landing distance, landing and take-off ground run, stalling speed, sinking speed, and gliding speed were determined.

The more important results of the analysis can be summarized as follows: The absolute minimum total take-off distance which was obtained with an airplane having a low wing loading and a moderately low aspect ratio is not reduced by the addition of boundary-layer control. The effectiveness of boundary-layer control in reducing the total take-off distance for a given maximum speed improves with increasing aspect ratio, and, for wing loadings of 10 pounds per square foot or more and an aspect ratio of 10 or more, the addition of boundary-layer control results in a decrease in the total take-off distance of as much as 14 percent. The total landing distance for a given maximum speed is reduced for all configurations by the use of boundary-layer control. The reduction varies from 25 to 40 percent depending on the wing loading.

The reduction in ground run for take-off was negligible for an aspect ratio of 5 but was of the order of 10 to 30 percent for aspect ratios of 10 and 15; whereas, the reduction in ground run for landing was from 25 to 40 percent for all configurations. The stalling speed for a given maximum speed was reduced 20 to 25 percent for all configurations by the application of boundary-layer control.

For the landing condition, boundary-layer control also reduced the gliding speed but resulted in a slightly higher sinking speed, or vertical velocity, than that for the conventional airplane having the same wing span.

INTRODUCTION

The design of a new airplane usually involves a compromise between several desired high-speed performance characteristics and the practical necessity for operating the airplane in and out of airports of reasonable size. The degree of necessary compromise has been reduced by the use of high-lift devices to increase the maximum lift coefficient. Such devices as leading- and trailing-edge flaps which are now in use on operational aircraft permit the attainment of maximum airplane lift coefficients, power-off, of the order of 2.8 (reference 1). In the belief that much higher airplane maximum lift coefficients would be desirable, numerous wind-tunnel investigations have been made of the effectiveness of boundary-layer control as a means for obtaining high maximum lift coefficients. Airfoil-section maximum lift coefficients as high as 5.5 have been obtained in wind-tunnel tests (see, for example, reference 2), and in a limited flight investigation airplane lift coefficients of 4.2 were obtained (reference 3).

There is, however, some question as to the exact benefits to be derived from the use of the high lift coefficients available with boundary-layer control. In an effort to obtain some idea of the extent to which the high lift coefficients available with boundary-layer control might be useful, an analytical investigation has been made of the effect of lift coefficient on the distance required for a four or five place or liaison type of airplane to take off and land over a 50-foot obstacle.

A liaison type of airplane was selected for the analysis since such an airplane might be expected to operate from small or makeshift airports where take-off and landing distances would be of primary importance. A 1,500-pound pay load and sufficient fuel for a 5-hour flight were assumed. The power, wing span, and aspect ratio of the airplane configurations investigated were varied over a wide range.

[1] Supersedes NACA TN 1597, "Analysis of the Effects of Boundary-Layer Control on the Take-Off Performance Characteristics of a Liaison-Type Airplane" by Elmer A. Horton and John H. Quinn, Jr., 1948, and NACA TN 2143, "Analysis of the Effects of Boundary-Layer Control on the Power-Off Landing Performance Characteristics of a Liaison-Type Airplane" by Elmer A. Horton, Laurence K. Loftin, Jr., and Stanley F. Racisz, 1950.

Allowances were made for changes in the gross weight resulting from changes in the airplane configuration and for the weight of the boundary-layer-control equipment. A maximum lift coefficient of 2.8 was assumed for the airplanes without boundary-layer control and a value of 5.0 was assumed to be the highest maximum lift coefficient available with boundary-layer control.

In addition to calculations of the distance required to land and take off over a 50-foot obstacle, the ground-run distance corresponding to landing and take-off, stalling speed, gliding speed, and sinking speed were calculated for all the airplanes. The maximum speed of each airplane configuration was also calculated in order to provide some indication of the relation between high-speed performance and landing and take-off performance. The landing maneuver was assumed to be executed without the use of power.

SYMBOLS

W	airplane gross weight, pounds
w	weight of airplane components, pounds
g	acceleration due to gravity (assumed equal to 32.2), feet per second per second
T	thrust, pounds
T_0	static thrust, pounds
$T_{V_{max}}$	thrust at maximum velocity, pounds
S	wing area, square feet
θ	angle of flight path with respect to ground, degrees
V	velocity, feet per second
$\overline{V}$	average flight velocity during transition arc, feet per second $\left(\frac{V_G+V_s}{2}\right)$
D	total drag, pounds
C_D	airplane drag coefficient (D/qS)
D_0	wing profile drag, pounds
C_{D_0}	wing profile-drag coefficient (D_0/qS)
C_{D_i}	induced drag coefficient $(C_L^2/\pi Ae)$
L	total lift, pounds
C_L	airplane lift coefficient (L/qS)
C_{L_T}	lift coefficient that would be required for steady level flight at speed $\overline{V}$
$\Delta C_L=C_{L_{max}}-C_{L_T}$	
s	horizontal distance, feet
s_t	total take-off distance over 50-foot obstacle, feet
s_L	landing distance from 50-foot obstacle, feet
R	radius of transition arc, feet
q	dynamic pressure, pounds per square foot $\left(\frac{1}{2}\rho V^2\right)$
H	total pressure, pounds per square foot
C_P	pressure coefficient $\left(\frac{H_0-H_d}{q_0}\right)$
Q	quantity rate of flow, cubic feet per second
C_Q	quantity rate of flow coefficient (Q/SV_0)
P	brake horsepower
A	aspect ratio (b^2/S)
h	altitude at which flare is started, feet
b	span, feet
e	wing efficiency factor based on variation of spanwise loading from an elliptical loading with no ground effect (assumed equal to 0.9)
$A_P=\frac{T_0}{P}$ $B=\frac{2(T-T_0)}{P\rho V^2}$ $C=\frac{T_{V_{max}}}{P}$	constants for calculating propeller thrust
η	efficiency factor of blower (assumed equal to 0.9)
μ	ground or braking friction coefficient or both
ρ	mass density of air, slugs per cubic foot
γ	ratio of specific heats at constant volume and constant pressure (1.4 for air)
τ	time, seconds

Subscripts:

c	conventional airplane
BLC	boundary-layer-control airplane
0	free-stream conditions
d	conditions in boundary-layer-control duct
L	conditions at point of ground contact on landing
max	maximum
u	pay load
G	glide
F	float
g	ground conditions for take-off
1	conditions during ground run of airplane for take-off
R	ground conditions for landing
t	conditions at take-off of airplane
T	transition
s	stalling
opt	optimum conditions

METHOD OF ANALYSIS

In calculating the take-off and landing performance characteristics for the various airplanes, a number of basic assumptions were made concerning the airplane configurations, the aerodynamic characteristics of the wing both with and without boundary-layer control, the method of estimating the weight of the airplane and the auxiliary boundary-layer-control equipment, and the method used in performing the take-off and landing maneuvers. The final comparative results should be unaffected by these assumptions inasmuch as the same assumptions were used for both the conventional and boundary-layer-control airplanes, except for the assumptions concerning the weight of the boundary-layer-control equipment which, in this instance, are believed to be conservative. In general, the assumptions were compatible with data from existing airplanes.

AIRPLANE CONFIGURATION

The airplane was assumed to have a cantilever semimonocoque wing, rectangular in plan form, with airfoil sections tapering from a thickness-chord ratio of 0.18 at the root to 0.12 at the tip. The empennage area was considered to be $0.25S$. The fuselage frontal area F for the constant pay load w_u of 1,500 pounds was determined from the following equation obtained from reference 4:

$$F=0.15w_u^{2/3}$$

The dimensions of the fuselage and landing gear remained constant.

The propeller was considered to be fully automatic in order that maximum engine speed and power could be obtained at all airspeeds. The fuel and oil supplies were assumed sufficient for 5 hours of cruising at 60 percent of maximum power with a specific fuel consumption of 0.50 pound per brake horsepower per hour.

It was assumed that an auxiliary engine and a blower were used to apply suction through the duct provided by the internal space of the semimonocoque wing to the boundary-layer-control slots. The boundary-layer-control apparatus was assumed to have a fuel supply sufficient for the duration of the flight.

AERODYNAMIC CHARACTERISTICS

The variation of wing profile-drag coefficient with lift coefficient, shown in figure 1, was determined from section data contained in references 5 to 8. The data are for the smooth-surface condition of the wings with and without boundary-layer control. The use of boundary-layer suction is seen to cause only relatively small changes in the profile drag in the range of lift coefficients from 0 to 1.6. On a wing provided with suction slots to improve the maximum lift, however, suction through these slots must be maintained in the cruising range of lift coefficients in order that the profile drag will not be increased by outflow through the slots. For this reason, the previously mentioned provision of enough fuel to operate the boundary-layer-control apparatus continuously during the 5-hour flight was considered necessary. The use of a drag polar based on airfoil-section data for the rough-surface condition might represent a more realistic appraisal of the high-speed characteristics of the airplane configurations investigated. Enough data were not available, however, to permit the determination of the drag polar for the rough-surface condition. The assumed empennage drag coefficient based on the empennage area was 0.01 and the assumed fuselage and landing-gear drag coefficients were 0.20 and 0.05, respectively, based on the fuselage frontal area (reference 9). The induced drag coefficients were calculated from the equation

$$C_{D_i}=\frac{C_L^2}{\pi Ae}$$

where the value of e was assumed to be 0.9. The maximum attainable lift coefficients were assumed to be 2.8 and 5.0 for the airplane without and with boundary-layer control, respectively.

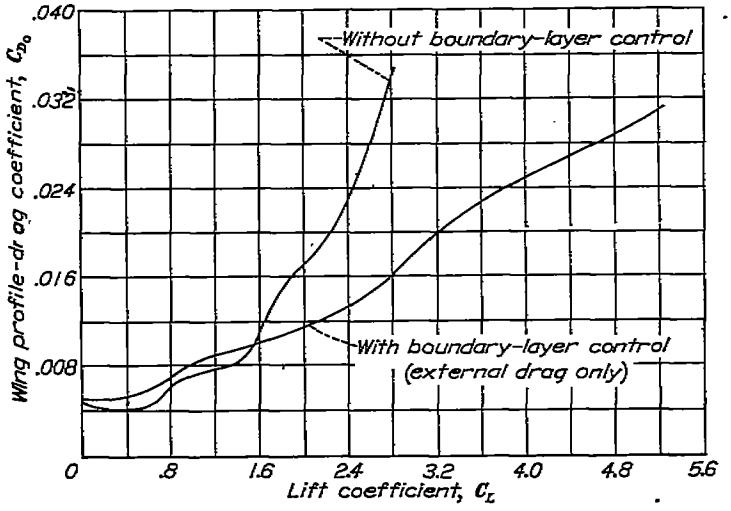

FIGURE 1.—Assumed profile-drag coefficient of the wing with and without boundary-layer control.

WEIGHT ANALYSIS

It was found convenient to express the gross weight of the airplane in terms of the wing span, aspect ratio, and power. The relation expressing the gross weight as a function of these variables was found by determining the weights of various airplane components as functions of one or more of the variables. The airplane components are designated by the following subscripts:

m	engine
p	propeller, hub, and engine auxiliaries
g	gasoline and oil
F	fuselage
L	landing gear
E	empennage
w	wing
b	blower
bm	blower engine

The following empirical relations giving the weights of engine, engine auxiliaries, propeller, and hub were determined from an analysis of 65 airplanes and 225 engines ranging from 50 to 2,000 horsepower (references 9 and 10):

$$w_m=P\left(\frac{192}{P-30}+1.1\right) \quad (1)$$

$$w_p=P\left(\frac{4.58}{P^{0.68}}+0.48\right) \quad (2)$$

The airplane was assumed to have a cruising duration of 5 hours at 60-percent full power with a specific fuel consumption of 0.5 pound per horsepower per hour and an oil requirement of 1 gallon per 16 gallons of gasoline (reference 9). Thus, the weight of gasoline and oil is

$$w_g=1.62P \quad (3)$$

The empirical relations giving the weight of fuselage, landing gear, empennage, and wing are from reference 9 and are as follows:

$$w_F=0.172W^{0.94} \tag{4}$$

$$w_L=0.067W^{0.98} \tag{5}$$

$$w_E=0.25S \tag{6}$$

$$w_w=0.046SA^{0.47}\left(\frac{W}{b}\right)^{0.53}\left(\frac{b}{t}\right)^{0.115} \tag{7}$$

For the analysis, a value of $\frac{b}{t}=35$, which is a representative value for the type airplane considered, was assumed in evaluating equation (7). The ratio of span to root thickness b/t enters in the wing weight equation to the 0.115 power and, since the wing weight is only approximately 15 percent of the gross weight, this ratio could vary appreciably without causing a change in the gross-weight estimate of more than 1 to 2 percent.

A summation of equations 1 to 7 plus the assumed pay load of 1,500 pounds results in the following empirical relation giving the gross weight of the conventional airplane as a function of span, aspect ratio, and horsepower:

$$W_c=P\left(\frac{192}{P-30}+\frac{4.58}{P^{0.68}}+3.20\right)+1500+0.172W^{0.94}+$$
$$0.067W^{0.98}+S\left[0.25+0.07A^{0.47}\left(\frac{W}{b}\right)^{0.53}\right] \tag{8}$$

The gross weight of the boundary-layer-control airplane is then the gross weight of the conventional airplane plus the gross weight of the blower engine w_{bm} and blower w_b; that is,

$$W_{BLC}=W_c+w_{bm}+w_b \tag{9}$$

The estimate of the blower-engine power was made in terms of the compression ratio, quantity flow, absolute entrance pressure, and blower efficiency by the following expression for an adiabatic gas flow:

$$P_{bm}=\frac{\frac{\gamma}{\gamma-1}H_dQ}{550\eta}\left[\left(\frac{H_0}{H_d}\right)^{\frac{\gamma-1}{\gamma}}-1\right] \tag{10}$$

Reference 2 indicated that sufficient boundary-layer control for a maximum lift coefficient of 5.0 could be obtained with a flow coefficient $C_Q=0.03$ and a pressure coefficient $C_P=4.0$. However, in order to make a conservative estimate of the weight of the boundary-layer-control equipment, a flow coefficient of 0.04 and a pressure coefficient of 15.0 (reference 11) were used and, by substitution, equation (10) becomes, for $\eta=0.9$,

$$P_{bm}=0.00367\left(H_0-3\frac{W}{S}\right)\sqrt{WS}\left[\left(\frac{H_0}{H_0-3\frac{W}{S}}\right)^{0.286}-1\right] \tag{11}$$

The blower-engine weight was then obtained by assuming an engine weight of 2.5 pounds per horsepower and a flight duration of 5 hours at 60-percent power with a specific fuel consumption of 0.5 pound per horsepower per hour. With these assumptions, the blower-engine weight, including fuel, is

$$w_{bm}=4P_{bm}$$
$$=0.0147\left(H_0-3\frac{W}{S}\right)\sqrt{WS}\left[\left(\frac{H_0}{H_0-3\frac{W}{S}}\right)^{0.286}-1\right] \tag{12}$$

The weight of the blower was obtained by assuming an axial-flow stator-rotor type constructed of aluminum alloy having a hub-to-tip ratio of 0.6 and an axial velocity of 400 feet per second. The outer casing was assumed to be 0.125 inch thick and 48 inches long, the rotor, blades, and shaft, to be equivalent to a disk 2 inches thick with a diameter 0.8 of the tip diameter, and the stator vanes, to be equivalent to a disk 0.25 inch thick with the same diameter as the complete rotor. With these assumptions, the blower-weight equation was developed and is as follows:

$$w_b=0.044\sqrt{WS}+1.13(WS)^{0.25} \tag{13}$$

TAKE-OFF PERFORMANCE ANALYSIS

Take-off maneuver.—The take-offs were assumed to be made at full power, with no head wind, and to consist of three phases: (1) an accelerated run on the ground at the attitude for least total resistance until the speed for take-off was reached; (2) the transition arc or period of change of the flight path from ground run to steady climb; and (3) steady climb to an altitude of 50 feet where take-off is considered complete. A sketch illustrating the assumed maneuver is presented in figure 2.

Equations for total take-off distance.—The following equation for the total take-off distance was obtained from reference 12 by combining the expressions giving the distance

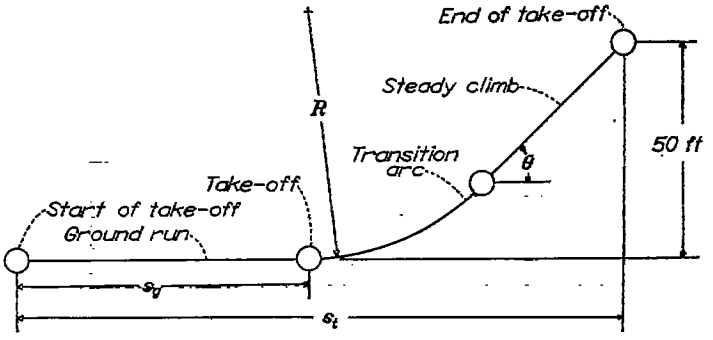

Airplane attitude	Condition
Ground run	From $V=0$ to $V=V_T$ C_{D_1}, C_{L_1}
Take-off	C_{L_2}, C_{D_2}, V_t

FIGURE 2.—Illustration of assumed maneuver to clear a 50-foot obstacle on take-off.

required for ground run, transition arc, and climb:

$$s_t=\frac{W/S}{\rho g}\left\{\frac{1}{(\mu C_{L_1}-C_{D_1})-B\frac{W/S}{W/P}}\log_e\left[1+\frac{(\mu C_{L_1}-C_{D_1})-B\frac{W/S}{W/P}}{\left(\frac{A_P}{W/P}-\mu\right)C_{L_t}}\right]+\frac{2\tan\frac{\theta}{2}}{C_{L_{max}}-C_{L_t}}+\frac{\rho g h}{\frac{W}{S}\tan\theta}\right\} \tag{14}$$

where

$$\theta=\sin^{-1}\left[\frac{A_P}{W/P}-\left(B\frac{W/S}{W/P}+C_{D_t}\right)\frac{1}{C_{L_t}}\right] \tag{15}$$

and

$$C_{L_t}=0.9\,C_{L_{max}}$$

which is the usual value assumed for C_{L_t} in an analysis of this nature.

The attitude of least air and ground resistance during the ground run, as shown in reference 13, is defined by the expression:

$$C_{L_1}=\frac{1}{2}\mu\pi Ae \tag{16}$$

In using equation (16) in the analysis, the profile-drag variation is neglected. The assumed ground friction coefficient $\mu=0.2$ is equivalent to that of deep grass or sand. A lower value of μ corresponding to that of concrete would reduce the take-off distance of both the conventional and boundary-layer-control airplanes by approximately the same percentage; thus the comparative results would be equal to those given in this report.

The power constants A_P and B used in equations 14 and 15 were obtained from reference 12 and are reproduced herein as figure 3. Use of figure 3 requires determination of V_{max} as a function of span, which was done by equating thrust to airplane drag as follows:

$$T_{V_{max}}=\frac{1}{2}\rho V_{max}^2\frac{b^2}{A}C_D \tag{17}$$

where C_D is the summation of the assumed drags of the airplane components in coefficient form. Also, from reference 12,

$$T_{V_{max}}=CP \tag{18}$$

where, from figure 3,

$$C=3.09-0.005\,V_{max} \tag{19}$$

equation (17) can then be expressed as

$$P(3.09-0.005\,V_{max})=\frac{1}{2}\rho V_{max}^2\frac{b^2}{A}C_D \tag{20}$$

From this equation V_{max} as a function of span for various powers and aspect ratios was obtained for both the conventional and boundary-layer-control airplane, and the results are given in figures 4 and 5. Once V_{max} is known as a function of span, the power constants A_P and B are obtained for the various spans from figure 3.

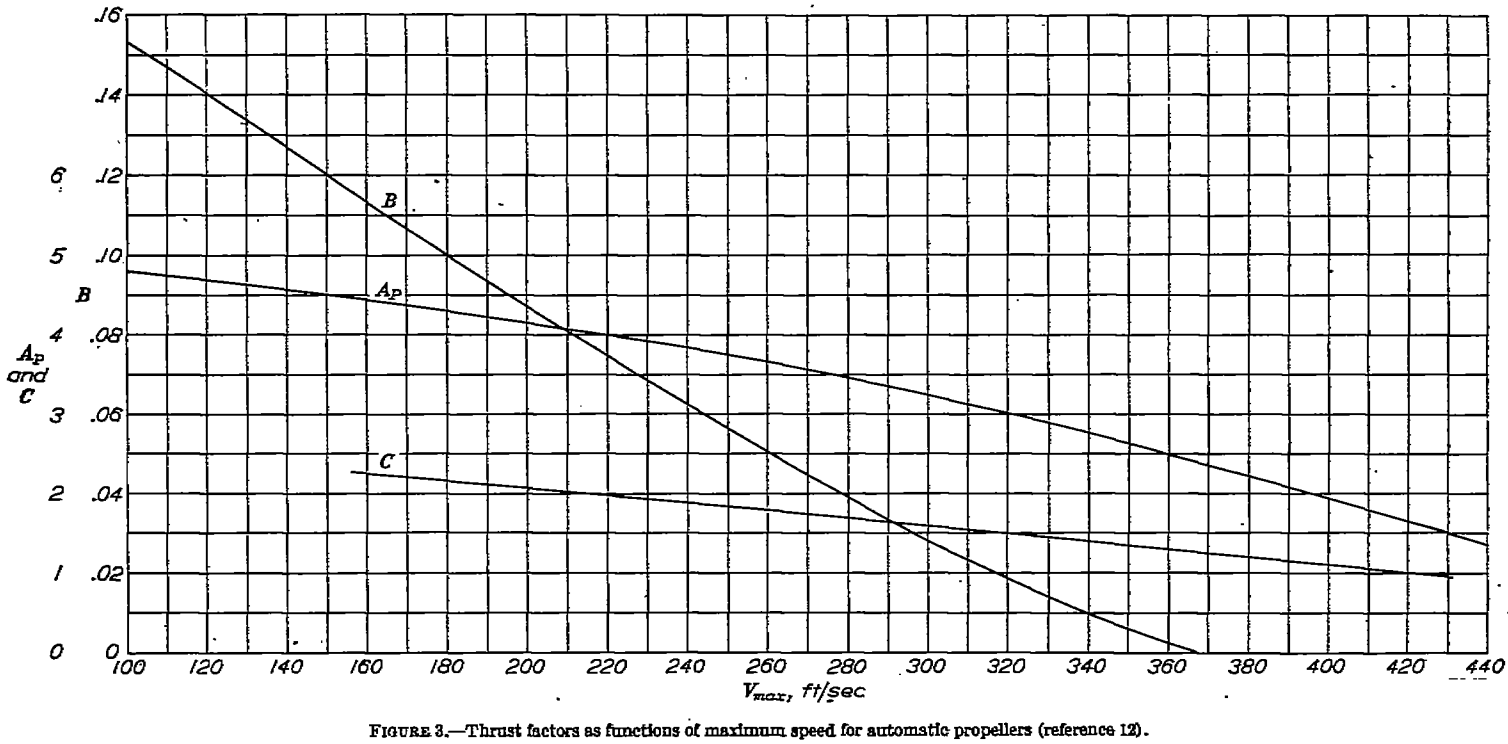

FIGURE 3.—Thrust factors as functions of maximum speed for automatic propellers (reference 12).

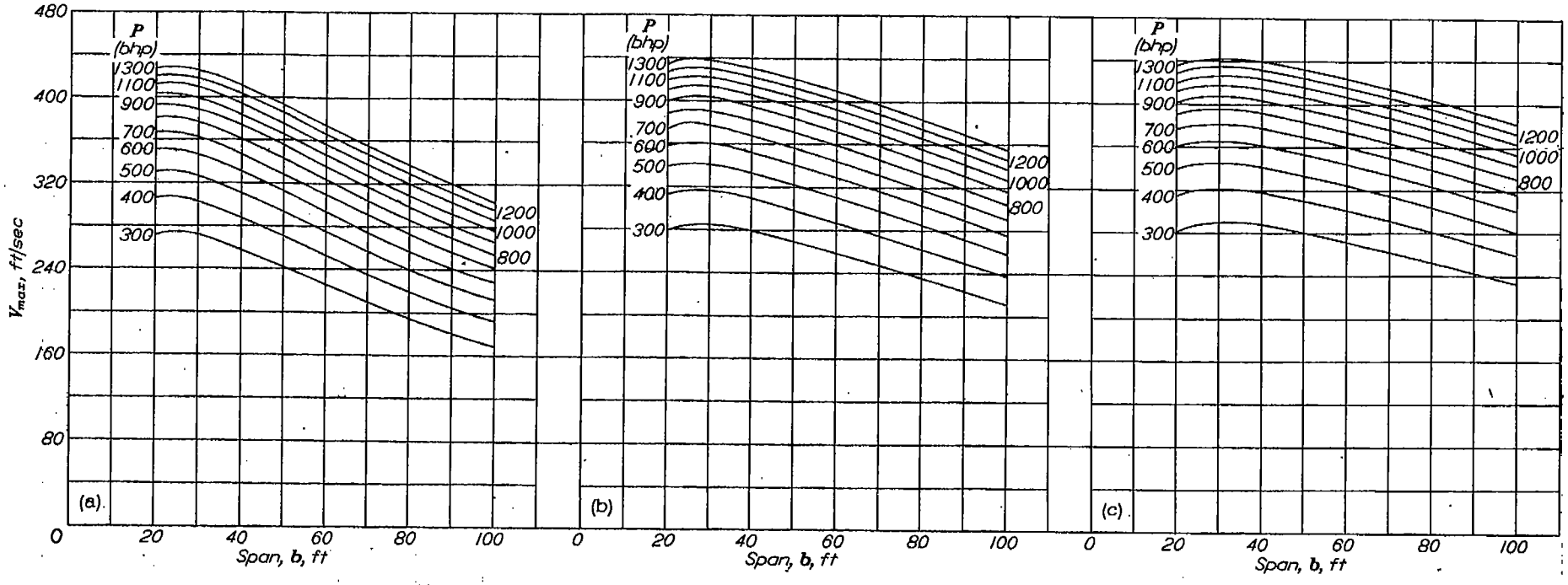

(a) $A=5$. (b) $A=10$. (c) $A=15$.

FIGURE 4.—Maximum speed of assumed airplane without boundary-layer control as a function of span for various powers.

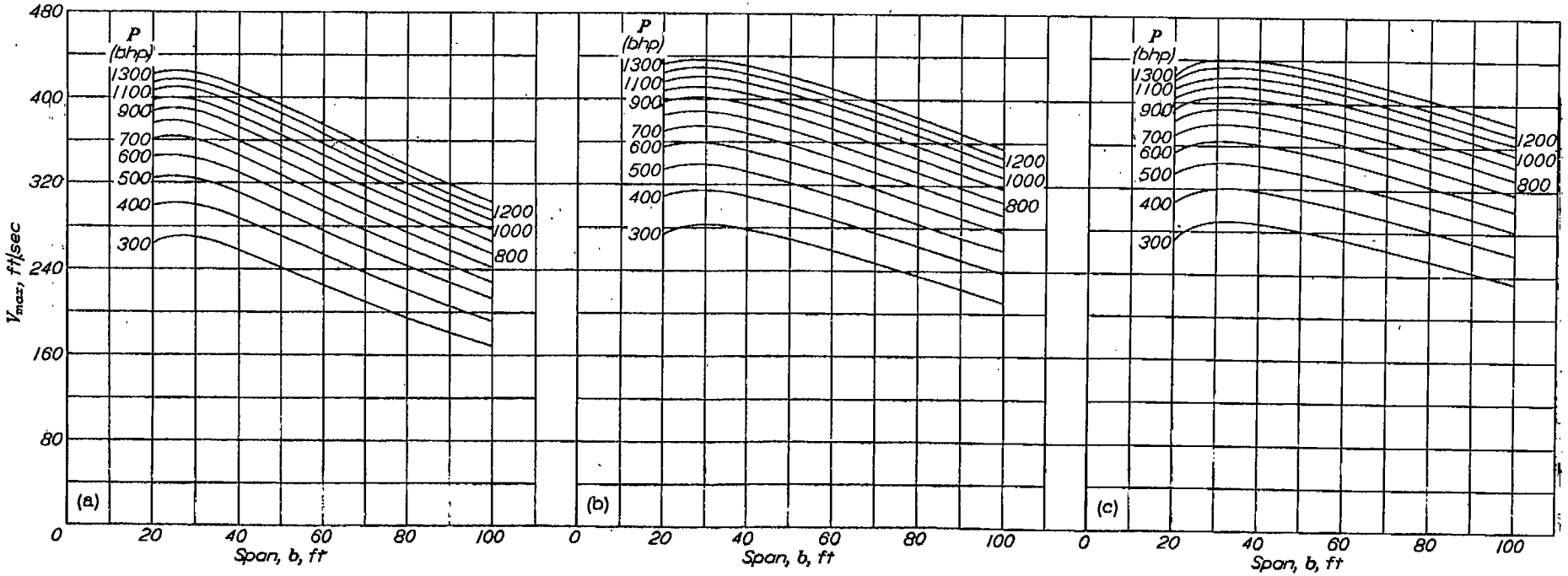

(a) $A=5$. (b) $A=10$. (c) $A=15$.

FIGURE 5.—Maximum speed of assumed airplane with boundary-layer control as a function of span for various powers.

Ground-run distance and stalling speed.—The ground run required for take-off was calculated by use of the following expression from reference 12:

$$s_g=\frac{W/S}{\rho g\left[(\mu C_{L_1}-C_{D_1})-B\frac{W/S}{W/P}\right]}\log_e\left[1+\frac{(\mu C_{L_1}-C_{D_1})-B\frac{W/S}{W/P}}{\left(\frac{A_P}{W/P}-\mu\right)C_{L_t}}\right] \tag{21}$$

The stalling speed V_s was found for each airplane from the relation

$$V_s=\sqrt{\frac{2W}{\rho S C_{L_{max}}}} \tag{22}$$

LANDING PERFORMANCE ANALYSIS

Landing maneuver.—The landing maneuver was considered to consist of four phases: (1) the steady glide, (2) a transition path executed at maximum lift coefficient to bring the airplane from a steady glide to level flight, (3) a floating period of 2 seconds to allow for lag in control response and for the application of brakes (see reference 14), and (4) the ground run. The beginning of the landing was considered as the point at which the altitude was 50 feet; the total landing distance was considered to be the horizontal distance from this point to the end of the ground run. The maneuver was considered to be performed without the use of power—that is, no propeller drag or thrust—and with no wind. A sketch illustrating the assumed maneuver is presented in figure 6.

Basic assumptions.—In calculating the total landing distance, certain simplifying assumptions were made in connection with the manner in which the transition from the steady-glide speed and attitude to level-flight speed and attitude was executed. These assumptions were based on the concept that the horizontal distance covered during the transition period for the type of airplane considered is a relatively small portion of the total landing distance so that a precise determination of the transition path is not required. The simplifying assumptions were:

1. The airplane was assumed to execute the transition at maximum lift coefficient and the transition path was assumed to be represented by an arc of constant radius. This assumption implies, of course, a constant speed during the transition.

2. Although a constant speed was assumed for the transition arc, it is, of course, obvious that in the actual case the speed during the transition must vary from the steady-glide speed to the landing speed. The constant speed implied by the assumption of a transition arc of constant radius was determined by assuming a linear variation in speed from the steady-glide speed to the stalling speed and taking the constant speed as the arithmetic mean of these two values. This assumption implies a constant decelerating force during the transition.

These assumptions are somewhat similar to those found in approximate methods for calculating the transition path following take-off (reference 12). Such approximate methods for calculating the take-off distance have been found to give good results and, in those cases for which experimental data were available, the method outlined for calculating the landing distance was also found to give good results.

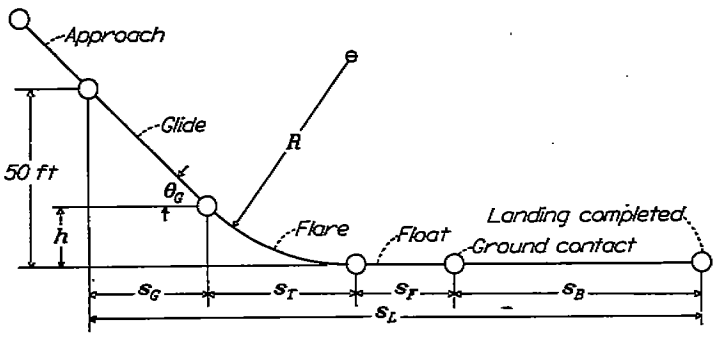

Airplane attitude	Conditions
Glide	V_G, C_{L_G}, C_{D_G}
Flare	V_T, C_{L_L}, C_{D_L}
Float	V_L, C_{L_L}, C_{D_L}
Ground contact	V_L, C_{L_L}, C_{D_L}
Landing completed.	$V=0$

FIGURE 6.—Illustration of assumed maneuver to clear a 50-foot obstacle in landing.

Development of landing equations.—On the basis of assumptions 1 and 2 the following equations for the total landing distance can be derived. The horizontal distance covered during the transition arc s_T is considered first. Reference to figure 6 shows that

$$s_T=R\sin\theta_G \tag{23}$$

where θ_G is the angle of steady glide and R is the radius of the transition arc. The instantaneous radius of curvature during a pull-up at maximum lift is given by the expression

$$R=\frac{2}{\rho g}\frac{W}{S}\frac{1}{C_{L_{max}}-C_{L_T}\cos\theta} \tag{24}$$

where C_{L_T} in this equation corresponds to the lift coefficient for unaccelerated level flight at the velocity at which the pull-up is being executed and θ is the instantaneous flight-path angle. If the cosine of the glide-path angle is assumed to be 1.0, equation (24) can be written as follows:

$$R=\frac{2}{\rho g}\frac{W}{S}\frac{1}{\Delta C_L} \tag{25}$$

where ΔC_L is the difference between the maximum lift coefficient and the lift coefficient corresponding to the previously defined mean speed used during the transition. Since the stalling speed is known, the value of the steady-glide speed V_G is all that is required for the determination of R and the horizontal distance covered during the transition. The value of V_G must be chosen in such a way that the time required for the velocity to decrease from V_G to V_L is the same as the time required for the airplane to traverse the distance s_T. The tangential forces acting on the airplane during the transition arc are composed of the drag which is a decelerating force and the component of weight along the flight path which is an accelerating force. The mean decelerating drag force

D_T is determined from the drag coefficient at the maximum lift coefficient and the mean speed $\overline{V}$.

There is, however, an accelerating force which may be determined in the following manner. At the end of the steady glide the following relation holds:

$$D_G = W \sin \theta_G$$

where D_G is the drag in the steady glide. Since the glide angle θ_G is usually small, θ varies in a nearly linear manner with s_T during the transition, and since $\sin \theta$ also varies in a nearly linear manner with θ for small values of θ, the mean accelerating force during the transition may be written as

$$\frac{W \sin \theta}{2} = \frac{D_G}{2}$$

Therefore, the time required for the airplane to decelerate from the steady-glide speed V_G to the landing speed V_L is then given by the following expression:

$$\tau = \frac{W}{g} \frac{V_G - V_L}{D_T - \frac{D_G}{2}} \tag{26}$$

If the cosine of the flight-path angle is considered to be unity, the time required to traverse the distance s_T is

$$\tau = \frac{s_T}{\overline{V}} \tag{27}$$

where $\overline{V}$ is the mean speed. Since the two intervals of time expressed by equations (26) and (27) must be equal, the distance s_T may be expressed in the following form:

$$s_T = \frac{2\overline{V}(V_G - V_L)W}{g(2D_T - D_G)} \tag{28}$$

If

$$\sin \theta_G = \sin \tan^{-1}\left(\frac{C_D}{C_L}\right)_G = \left(\frac{C_D}{C_L}\right)_G$$

the distance s_T as given by equations (23) and (25) may be written

$$s_T = \frac{2}{\rho g} \frac{W}{S} \frac{1}{\Delta C_L} \left(\frac{C_D}{C_L}\right)_G \tag{29}$$

A simultaneous solution of equations (28) and (29) gives, after some algebraic manipulation, the following equation:

$$\left[\left(\frac{C_D}{C_L}\right)_L \left(\frac{C_D}{C_L}\right)_G - 6\right]\left(\frac{V_L}{V_G}\right)^3 + \left[3\left(\frac{C_D}{C_L}\right)_G \left(\frac{C_D}{C_L}\right)_L + 10\right]\left(\frac{V_L}{V_G}\right)^2 + \left[\left(3 - 2\frac{C_{D_G}}{C_{D_L}}\right)\left(\frac{C_D}{C_L}\right)_G \left(\frac{C_D}{C_L}\right)_L - 2\right]\left(\frac{V_L}{V_G}\right) + \left[\left(1 - 2\frac{C_{D_G}}{C_{D_L}}\right)\left(\frac{C_D}{C_L}\right)_G \left(\frac{C_D}{C_L}\right)_L - 2\right] = 0 \tag{30}$$

An exact solution of equation (30) for $\frac{V_L}{V_G}$ requires additional analytic expressions relating $\left(\frac{C_D}{C_L}\right)_G$ and $\frac{C_{D_G}}{C_{D_L}}$ to $\frac{V_L}{V_G}$. Such relations can, of course, be found by expressing the drag polars for the various airplanes in analytic form. It was found more convenient, however, to perform a simultaneous solution of equations (28) and (29) by a trial and error process. Once the correct value of V_G is determined from equations (28) and (29), the horizontal distance covered in the transition arc is easily calculated for a particular airplane from equation (29).

The horizontal distance s_G, covered in the steady glide from a height of 50 feet to the height h at which the transition is begun, can be calculated by the following equations (see fig. 6):

$$s_G = \frac{50 - h}{\tan \theta_G} = \frac{50 - h}{\left(\frac{C_D}{C_L}\right)_G}$$

However,

$$h = R(1 - \cos \theta_G)$$

so that

$$s_G = \frac{50 - R\left[1 - \cos \tan^{-1}\left(\frac{C_D}{C_L}\right)_G\right]}{\left(\frac{C_D}{C_L}\right)_G} \tag{31}$$

The values of R and $\left(\frac{C_D}{C_L}\right)_G$ are already known from the previous calculations of the transition path so that s_G may be readily determined. The distance covered during the floating period is merely

$$s_F = 2V_L = 2\sqrt{\frac{2W}{\rho S C_{L_{max}}}} \tag{32}$$

The equation for determining the ground run or braking distance, obtained from reference 15, is

$$s_B = \frac{V_L^2}{2g\left(\frac{C_D}{C_L} - \mu\right)} \log_e \left(\frac{C_D/C_L}{\mu}\right) \tag{33}$$

where $\frac{C_D}{C_L}$ is the lift-drag ratio for the maximum-lift condition and V_L corresponds to the stalling speed. The combined ground and braking friction coefficient was assumed to be 0.4. This value of the friction coefficient can be obtained with cinders on ice. (See reference 14.) The ground effect on the induced drag was neglected. The total landing distance is obtained from a summation of the horizontal distances covered during the four phases of the maneuver:

$$s_L = s_G + s_T + s_F + s_B \tag{34}$$

where these four components are calculated by means of equations (31), (29), (32), and (33), respectively.

SCOPE OF CALCULATIONS

The landing and take-off performance characteristics calculated included the total landing and take-off distances, the ground run corresponding to landing and take-off, the stalling speed, the gliding speed, and the sinking speed. The airplanes for which the landing and take-off performances were calculated had wing spans varying from 25 feet to 100 feet, engine brake horsepowers varying from 300 to 1,300, and aspect ratios of 5, 10, and 15. As previously stated, the wing span, aspect ratio, and power determine the weight of an airplane and the airplane configuration. The actual values of the engine horsepower for which calculations were made were somewhat different for the landing and take-off analysis; however, the range of horsepowers covered in the two analyses was the same. The landing and take-off performances were calculated for each airplane with and without boundary-layer control. The highest attainable value of the maximum lift coefficient was assumed to be 2.8 for the airplanes without boundary-layer control and, 5.0 for the airplanes with boundary-layer control. The landing performance calculations were made only for lift coefficients of 2.8 and 5.0. The take-off performance calculations, however, were made for a number of lift coefficients in order to determine the optimum value for each configuration. The effect of the additional weight of the boundary-layer-control equipment on the take-off performance characteristics was isolated by calculating the take-off performance characteristics of the boundary-layer-control airplane with and without the additional weight of the boundary-layer-control equipment included in the gross-weight estimate. This calculation was made for wings of aspect ratio 10 only inasmuch as the effect would be relatively the same for other aspect ratios.

Data defining the range of airplane configurations for which the performance calculations were made are presented in figures 7 and 8 for the airplanes without and with boundary-layer control, respectively. These data were obtained by cross-plotting the data derived from equations 8, 12, and 13, examples of which are given in figures 9 and 10 for the aspect-ratio-10 configuration. From figures 7 and 8 it is seen that the wing loading of the airplanes investigated varied from about 4 pounds per square foot to 160 pounds per square foot without boundary-layer control and, from 4 pounds per square foot to 180 pounds per square foot with boundary-layer control.

The maximum velocity of the different airplane configurations without and with boundary-layer control was calculated in order to provide a basis of comparison for the high- and low-speed performances and is given in figures 4 and 5. From figures 4 and 5 it is seen that for a given wing span, aspect ratio, and brake horsepower of the main propulsive unit the maximum velocities of the airplanes with and without boundary-layer control are nearly the same. The slight variation in speed is due to the additional weight of the boundary-layer-control equipment which increases the wing loading and thus the lift and drag coefficient for any given speed and also the small extent to which the drag polars of the airplanes with and without boundary-layer control differ in the low lift-coefficient range (fig. 1).

RESULTS AND DISCUSSION

The discussion is intended to show the effects of increasing the maximum lift coefficient by boundary-layer control upon the landing and take-off performance characteristics and upon the relation between high-speed performance and the take-off and landing performance as the airplane configuration is varied. The pertinent take-off and landing performance characteristics are presented in terms of the wing span, power, and aspect ratio for the airplanes with and without boundary-layer control. The choice of variables employed in presenting the data was arbitrary to some extent. Although other parameters could have been employed, span, aspect ratio, and power were chosen because these variables indicate the physical size and practicability of the airplane. In some cases, the performance parameters were plotted against wing loading or power loading as well as wing span because their use tended to clarify the results. The effect upon the take-off characteristics of increasing the maximum lift coefficient by boundary-layer control is discussed first.

TAKE-OFF CHARACTERISTICS

The take-off characteristics to be discussed are:

(1) The total take-off distance

(2) The ground run and stalling speeds

TOTAL TAKE-OFF CHARACTERISTICS

Examples of the variations of total take-off distance of the boundary-layer-control airplane with maximum lift coefficient for various spans and horsepowers at an aspect ratio of 10 are presented in figure 11. For a given aspect ratio, the lift coefficient for minimum take-off distance increases as the span decreases and the wing loading increases. These results were cross-plotted in figure 12 to show the variation of optimum C_L with wing loading for the various aspect ratios and horsepowers. The figure shows that at an aspect ratio of 5, regardless of wing loadings, the optimum lift coefficient is less or slightly greater than that available with conventional high-lift devices. For aspect ratios of 10 and 15 and wing loadings of less than 10 pounds per square foot, although the optimum maximum lift coefficient for take-off exceeds the maximum lift coefficient attainable without boundary-layer control, the use of lift coefficients greater than 2.8 will decrease the take-off distance very little. (See fig. 11.) For the larger wing loadings, however, the rate of change of the take-off distance with lift coefficient is large and the use of the optimum lift coefficient offers a considerable decrease in take-off distance.

Throughout the remainder of the analysis, the effects of other variables on total take-off distance are discussed for the optimum lift coefficient unless it exceeds 5.0, in which case the take-off distance was calculated for a maximum lift coefficient of 5.0.

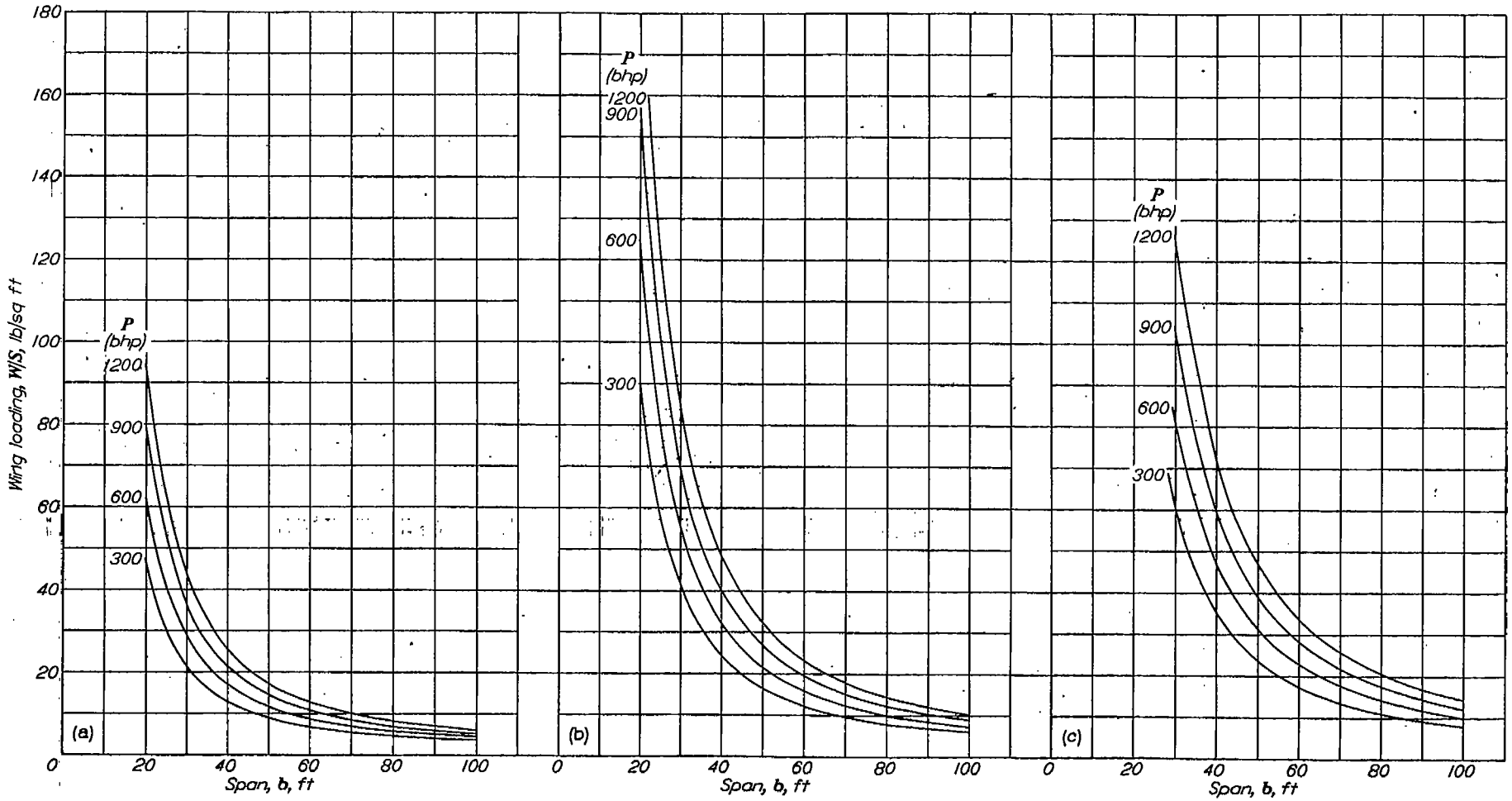

(a) $A=5$. (b) $A=10$. (c) $A=15$.

FIGURE 7.—Wing loading of assumed airplane without boundary-layer control as a function of span for various powers.

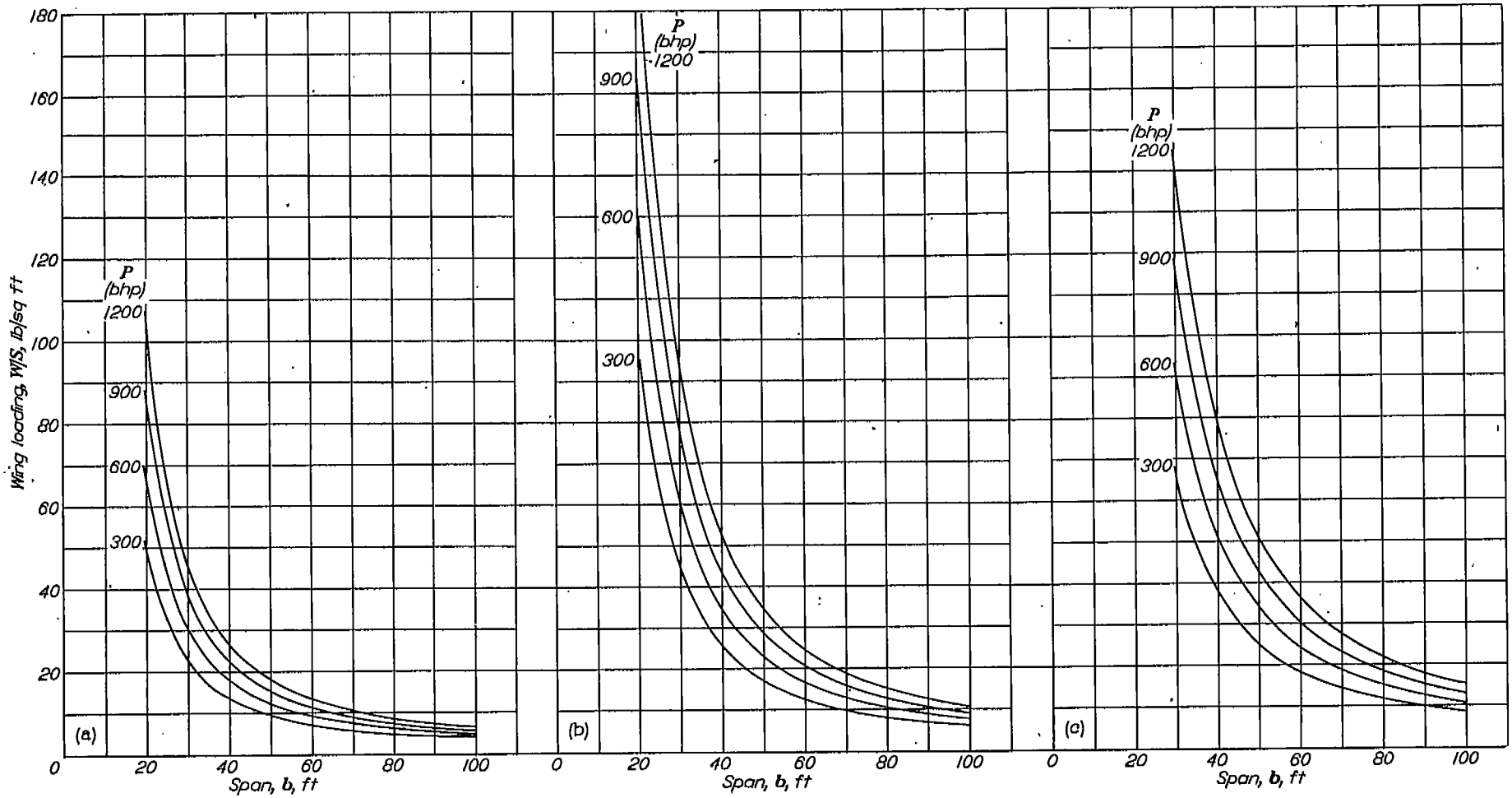

(a) $A=5$. (b) $A=10$. (c) $A=15$.

FIGURE 8.—Wing loading of assumed airplane with boundary-layer control as a function of span for various powers.

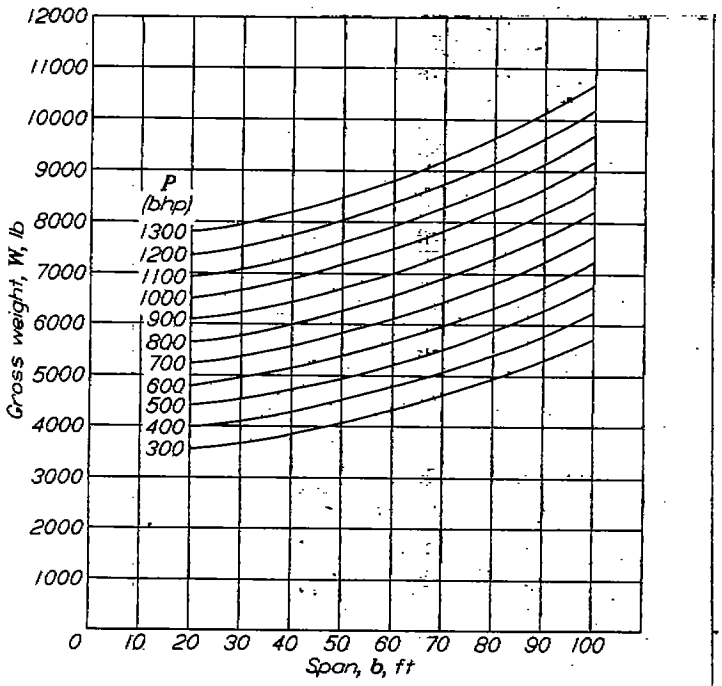

FIGURE 9.—Gross weight of conventional airplane as a function of span for various powers. $A=10$.

Effect of boundary-layer control on take-off.—The variation of take-off distance with span for various horsepowers is presented for aspect ratios of 5, 10, and 15 in figures 13 and 14 for the conventional and boundary-layer-control airplanes, respectively. The effect of the weight of the boundary-layer-control equipment on the take-off characteristics was found for an aspect ratio of 10 by assuming that no weight was added by the auxiliary blower and motor. These data are presented in figure 15.

The effect of boundary-layer control on the total take-off distance of the airplane may be seen in figure 16, which shows the total take-off distance as a function of maximum speed for both the conventional and boundary-layer-control airplanes with varying aspect ratio and horsepower. Figure 16 shows that for a given maximum speed and an aspect ratio of 5, regardless of span, the boundary-layer-control airplane generally requires more distance for take-off than the conventional airplane. As the aspect ratio increases, however, boundary-layer control becomes more effective, and for an aspect ratio of 10 or more with a wing loading of 10 pounds per square foot or more the addition of boundary-layer control decreases the total take-off distance. It follows that, for a given take-off distance, the boundary-layer-control airplane would have a greater maximum speed.

The effect of the weight of the boundary-layer-control equipment on the total take-off distance is shown in figure 16 (b) for aspect ratio of 10. This figure shows that the total take-off distance may be decreased appreciably by decreasing the weight; therefore, every effort should be made to decrease the weight of the boundary-layer-control equipment.

Figure 16 also shows that the absolute minimum total take-off distance obtained with a low wing loading and moderately low aspect ratio is not decreased by the addition of boundary-layer control.

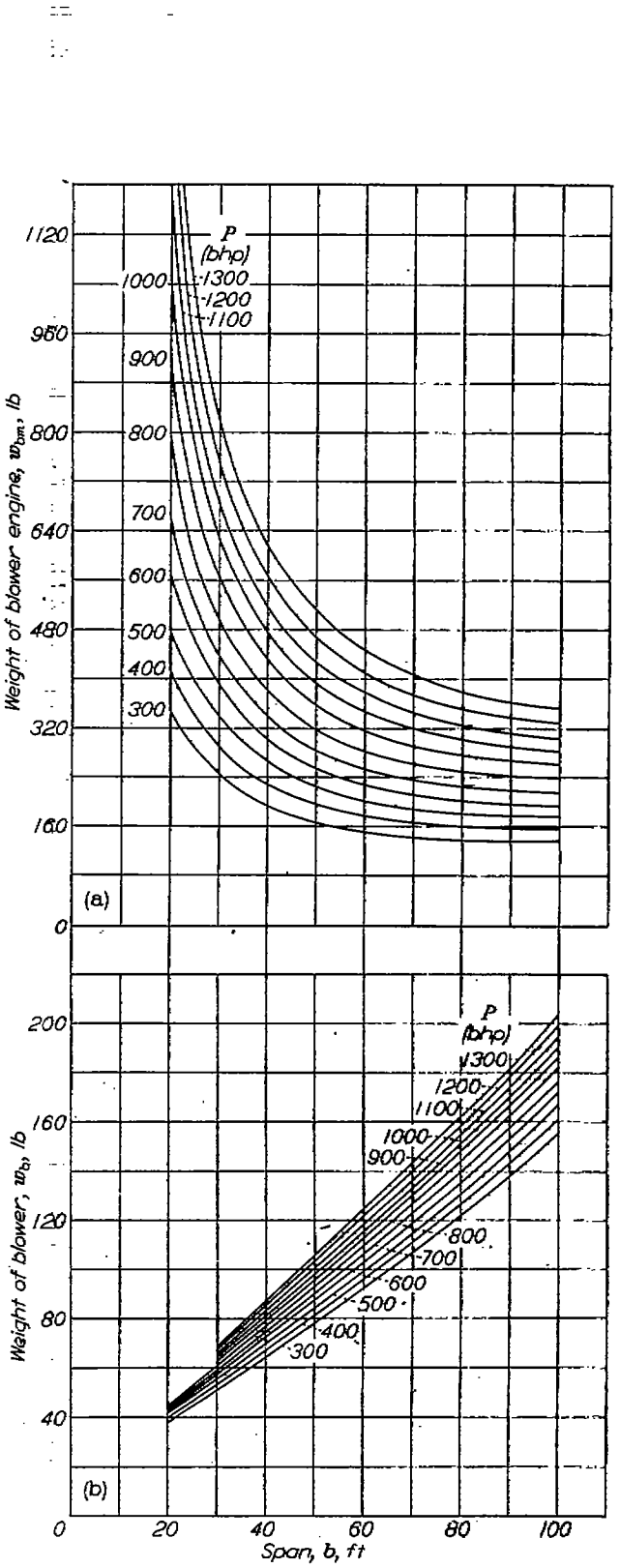

(a) Weight of blower engine.
(b) Weight of blower.

FIGURE 10.—Weight of boundary-layer-control equipment as a function of span for various main engine powers. $A=10$.

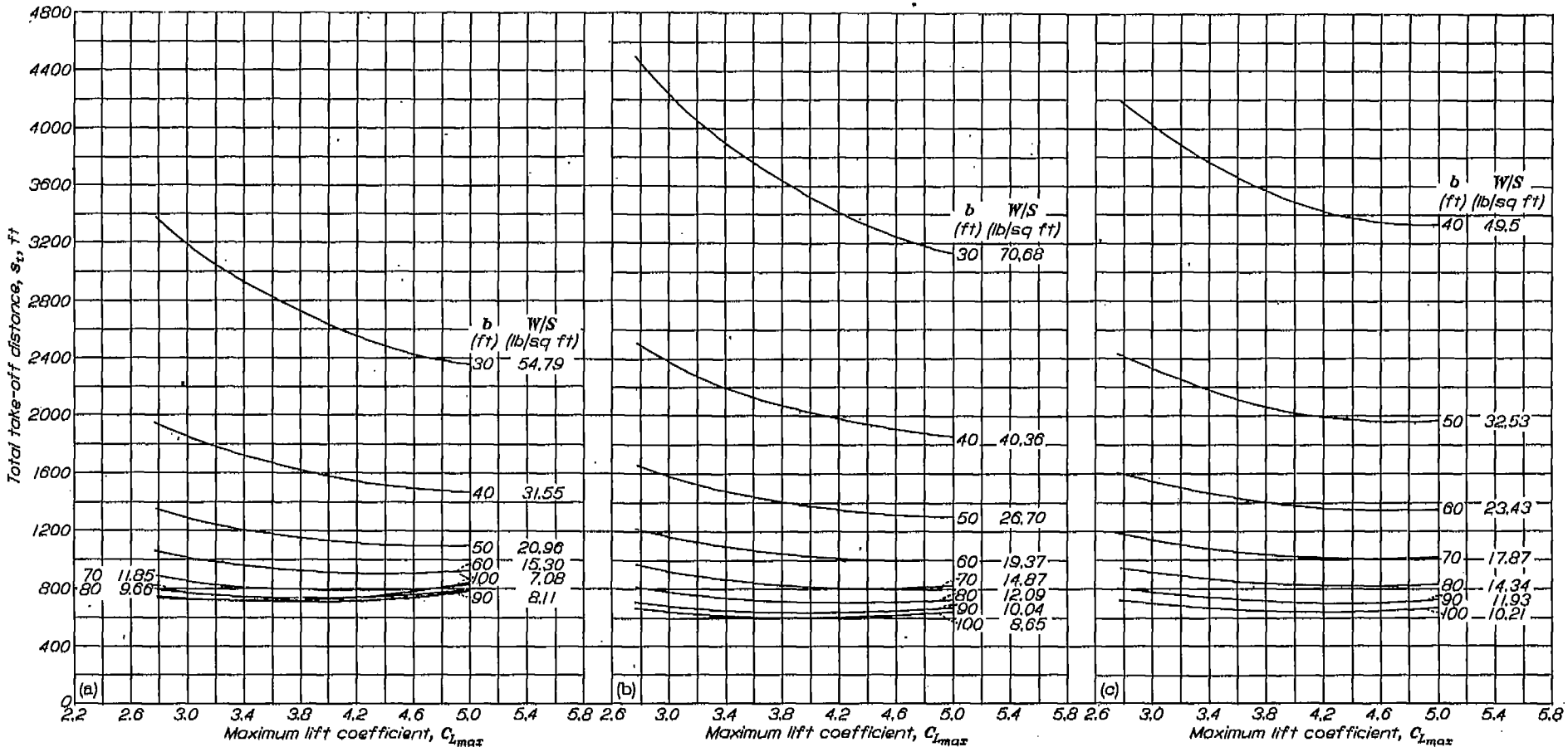

(a) P=500 bhp. (b) P=800 bhp. (c) P=1100 bhp.

FIGURE 11.—Total take-off distance of an airplane with boundary-layer control as a function of maximum lift coefficient for various spans and wing loadings. A=10.

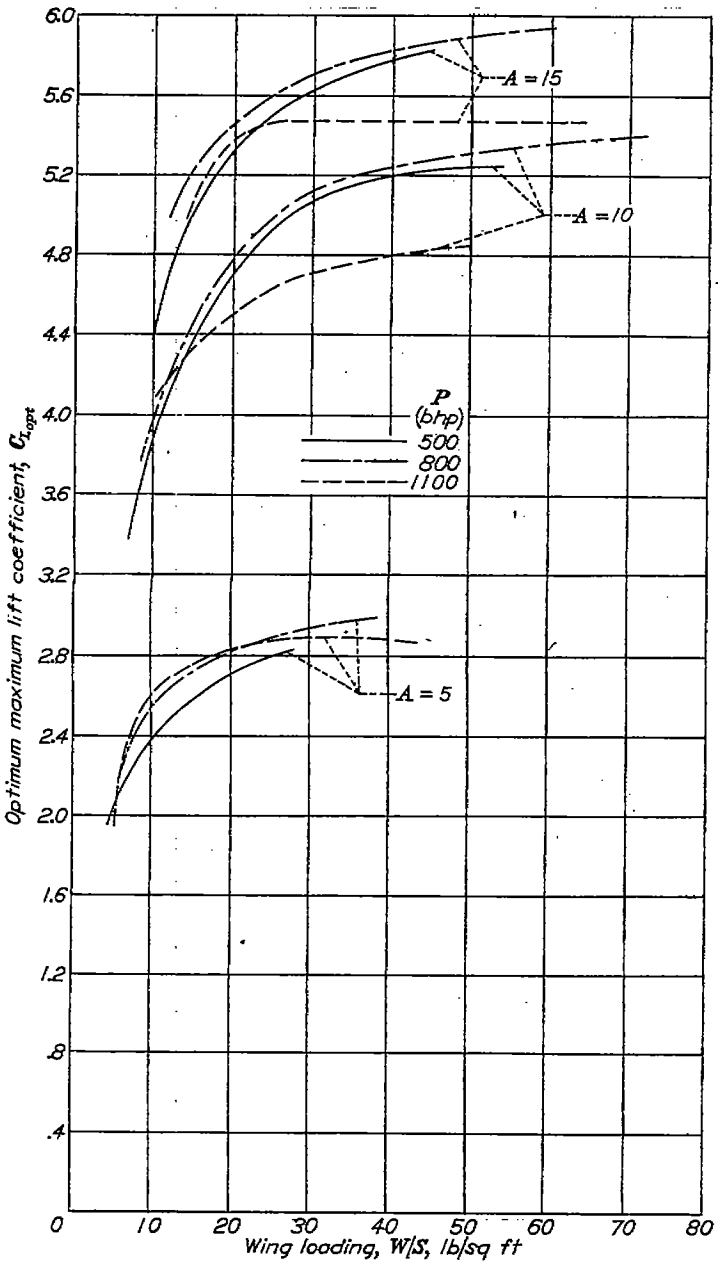

FIGURE 12.—Optimum maximum lift coefficient for minimum total take-off distance of an airplane with boundary-layer control as a function of wing loading for various aspect ratios and powers.

Effect of power loading on take-off distance.—The power loading is shown as a function of take-off distance for various wing loadings and aspect ratios in figures 17 and 18 for the conventional and boundary-layer-control airplanes, respectively. As is shown, the optimum power loading, which is nearly independent of wing loading and aspect ratio, is approximately 8.5 and 9.0 pounds per horsepower for the conventional airplane and the boundary-layer-control airplane, respectively. It should be noted that increasing the horsepower above the optimum value increases the take-off distance. This result is due to the accompanying change in engine, fuel, and structural weight.

GROUND-RUN AND STALLING-SPEED CHARACTERISTICS

In order to obtain the minimum ground run, which is given in figures 19 and 20, the calculations were made by considering the ground run completed when a speed was reached corresponding to a flying speed at 0.9 of the assumed maximum lift coefficient. During the analysis, it was found that, because the induced drags were large for aspect ratio of 5 of the boundary-layer-control airplane, the power was insufficient to maintain level flight at lift coefficients greater than 3.8; therefore, the ground run for an aspect ratio of 5 was calculated for a maximum lift coefficient of 3.8. The variation of ground run with span for various horsepowers and aspect ratios is shown in figures 19 and 20 for the conventional and boundary-layer-control airplanes, respectively, and in figure 21 for the airplane with boundary-layer control but with the weight of the additional equipment disregarded. These data are compared in figure 22 where the ground run has been plotted as a function of V_{max} for various horsepowers and aspect ratios.

The boundary-layer-control airplane had shorter ground runs than the conventional airplane for all configurations considered. The reduction was negligible for an aspect ratio of 5 and a maximum lift coefficient of 3.8. At aspect ratios of 10 and 15 and maximum lift coefficient of 5.0, however, the ground run was decreased 10 to 30 percent by the addition of boundary-layer control. The beneficial effect of reducing the boundary-layer-control-equipment weight, as previously noted for the total take-off distance, was again observed for the case of the ground run (fig. 22 (b)).

This reduced ground run produced by use of high maximum lift coefficients associated with boundary-layer control may prove to be most advantageous for carrier-based airplanes or seaplanes.

The stalling speed V_s is presented as a function of maximum speed in figure 23 for various aspect ratios and horsepowers. The stalling speed was 20 to 25 percent less for the boundary-layer-control airplane than for the conventional airplane for all configurations considered.

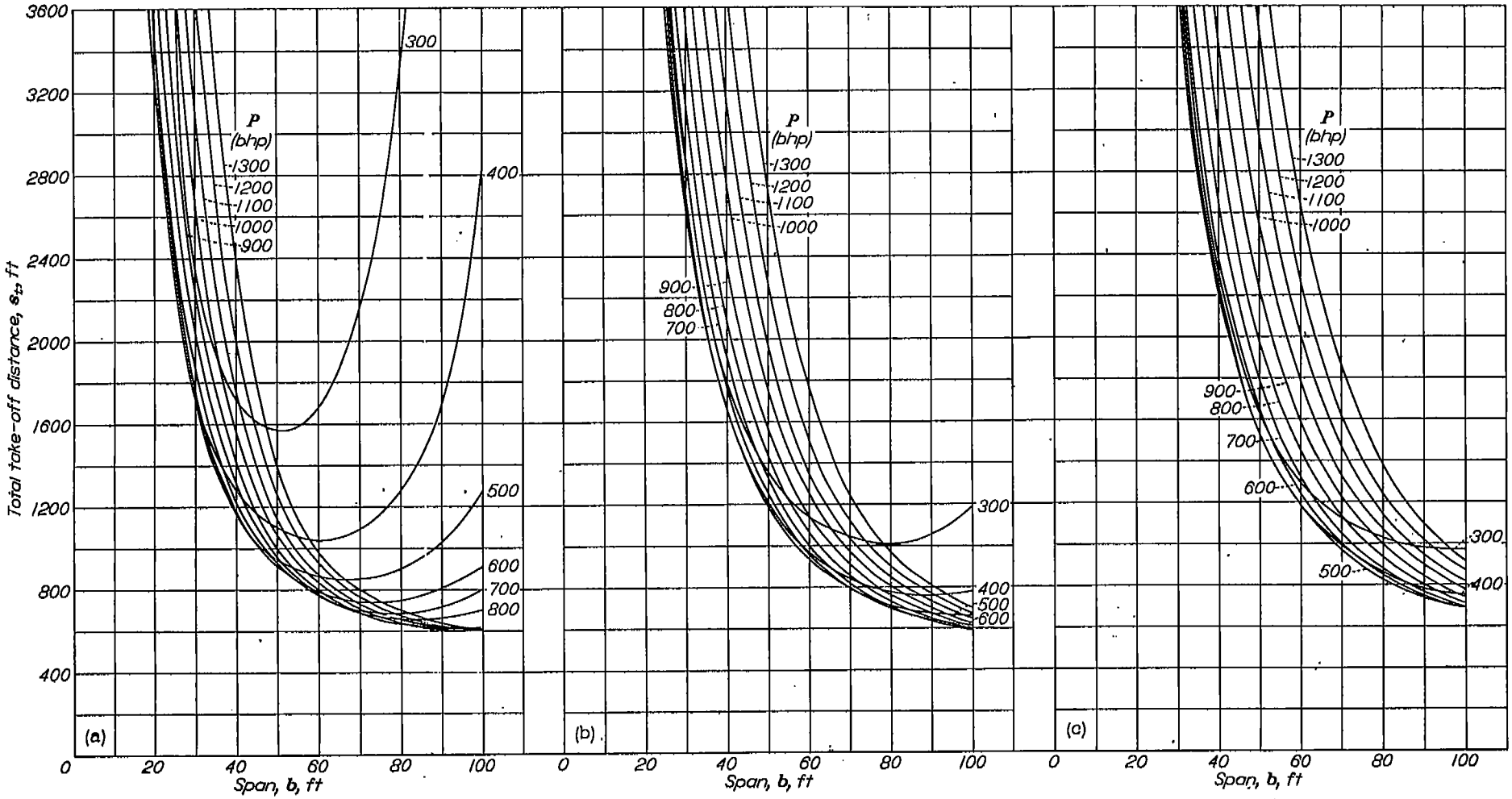

(a) $A=5$. (b) $A=10$. (c) $A=15$.

FIGURE 13.—Total take-off distance of an airplane without boundary-layer control as a function of span for various powers.

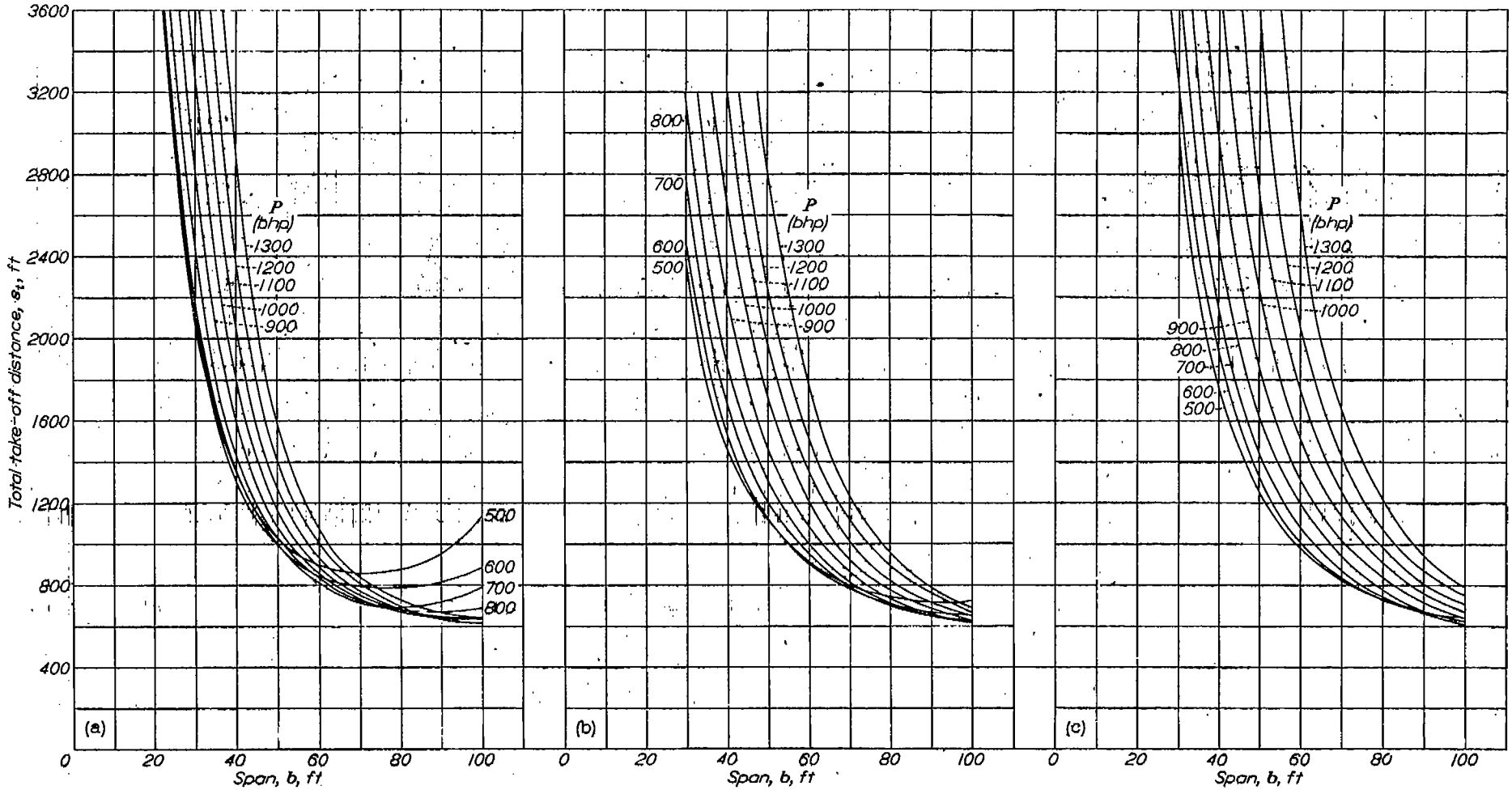

(a) $A=5$. (b) $A=10$. (c) $A=15$.

FIGURE 14.—Total take-off distance of an airplane with boundary-layer control as a function of span for various powers.

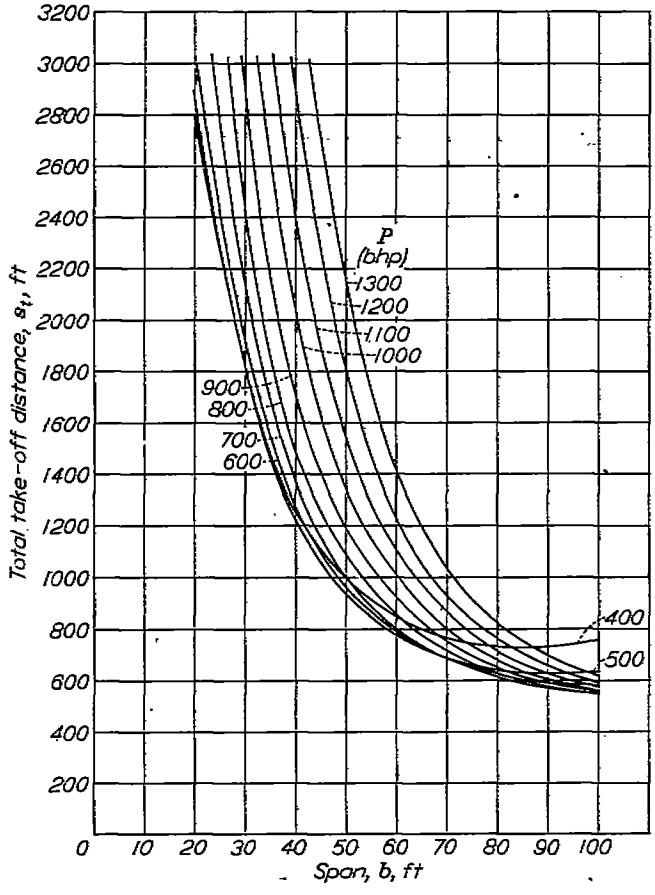

FIGURE 15.—Total take-off distance of an airplane with boundary-layer control, but with weight of boundary-layer control equipment excluded, as a function of span for various powers. $A=10$.

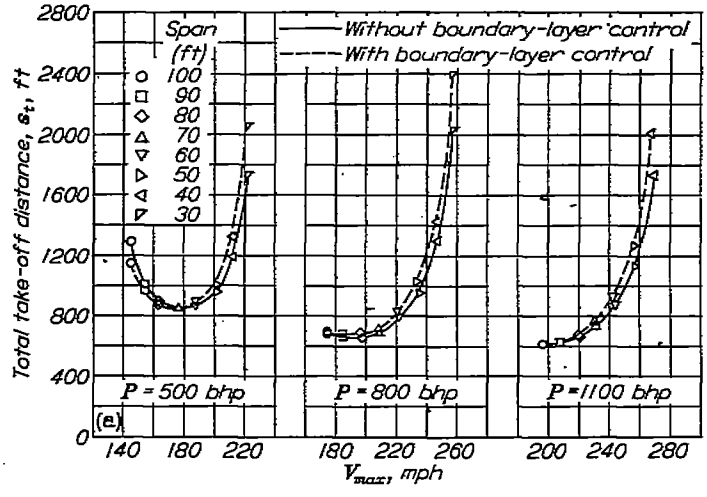

(a) $A=5$.

FIGURE 16.—Total take-off distance of an airplane with and without boundary-layer control as a function of maximum speed for various powers.

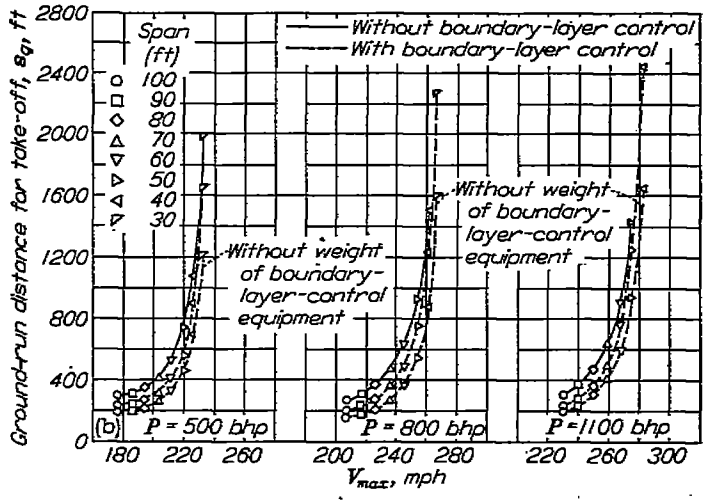

(b) $A=10$.

FIGURE 16.—Continued.

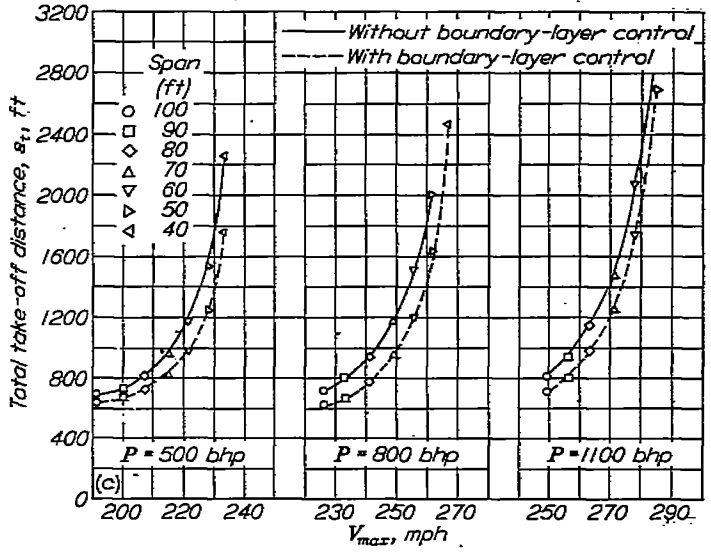

(c) $A=15$.

FIGURE 16.—Concluded.

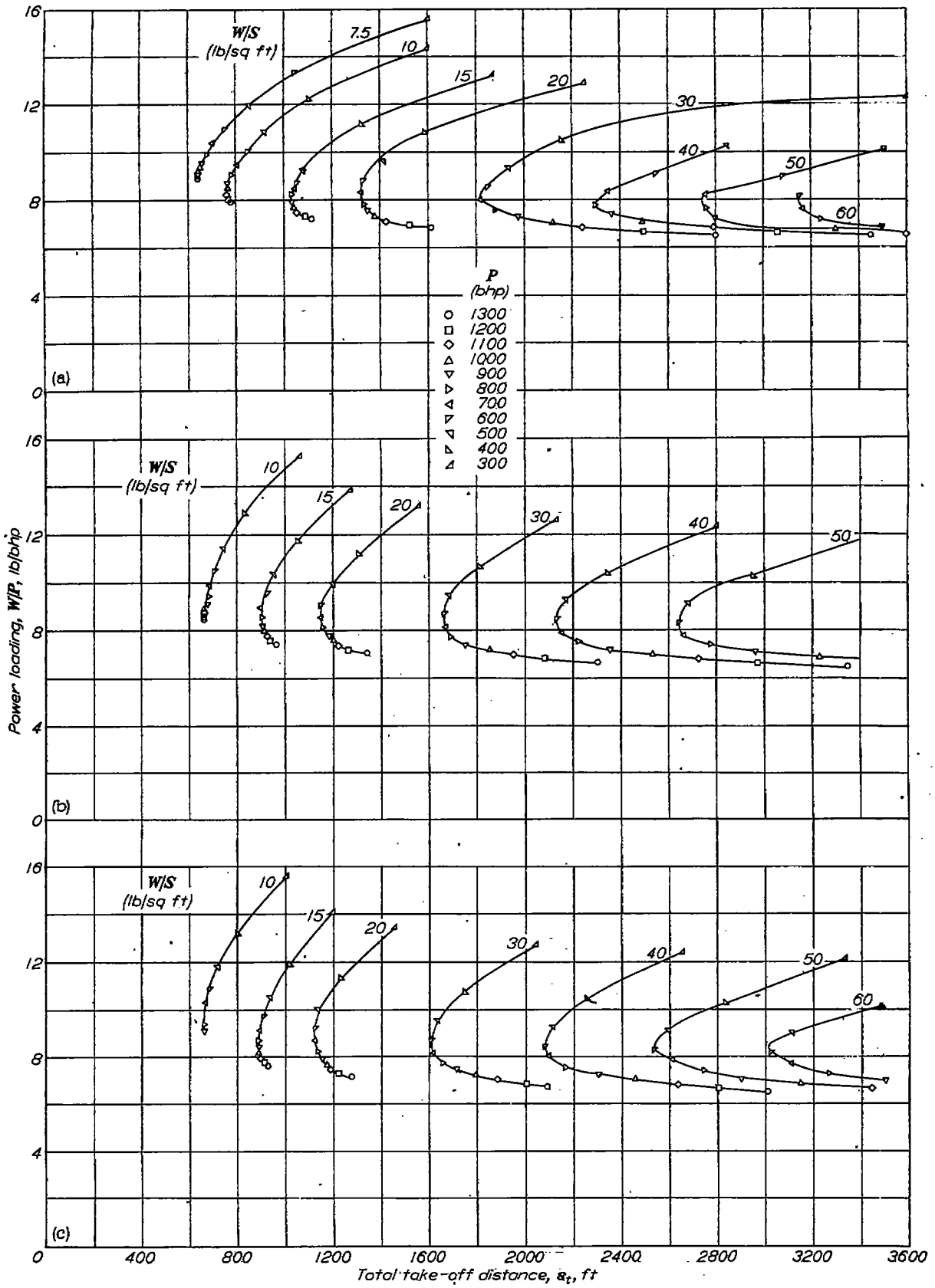

(a) $A=5$.
(b) $A=10$.
(c) $A=15$.

FIGURE 17.—Total take-off distance of an airplane without boundary-layer control as a function of power loading for various wing loadings.

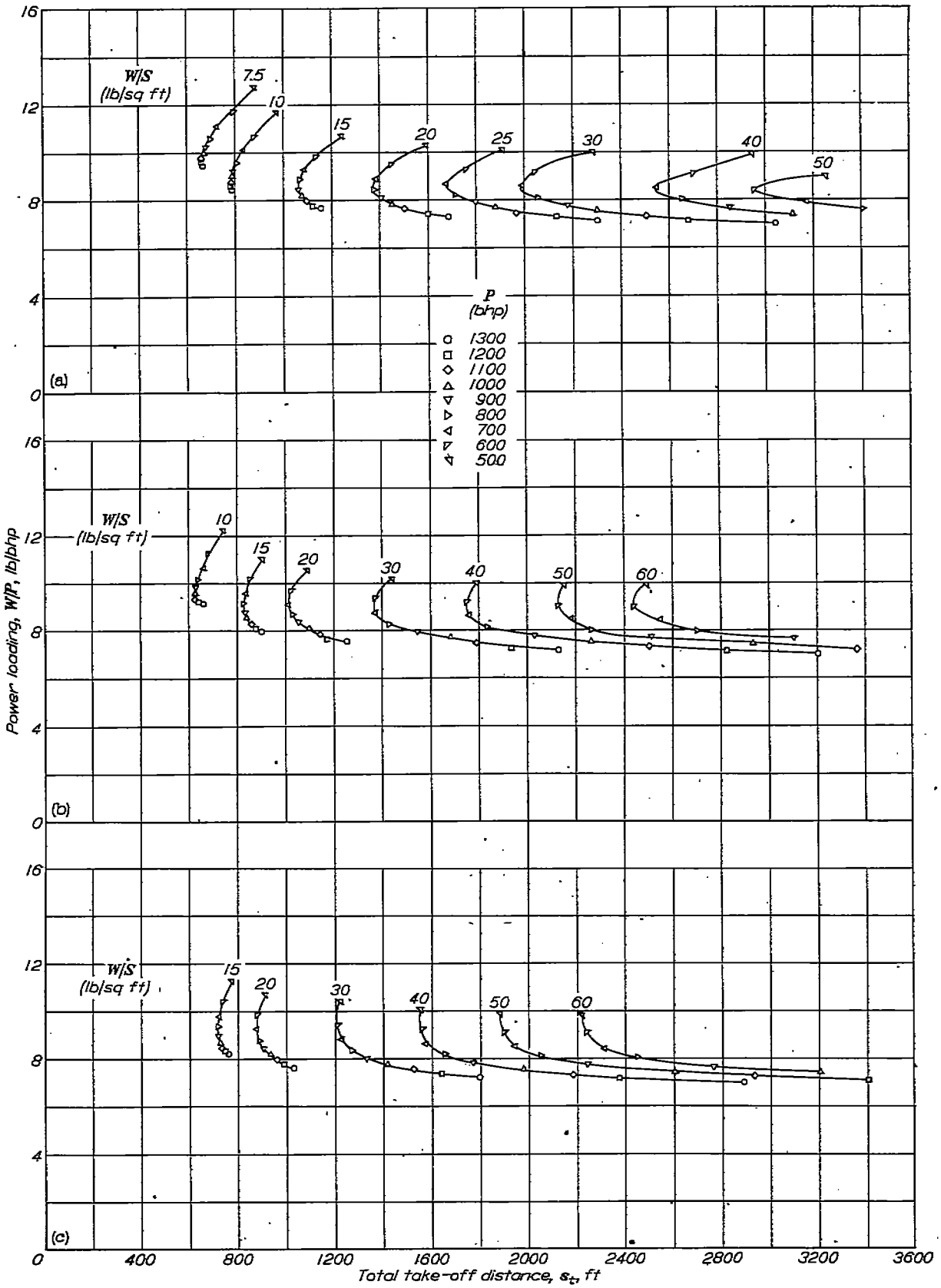

(a) A=5.
(b) A=10.
(c) A=15.

FIGURE 18.—Total take-off distance of an airplane with boundary-layer control as a function of power loading for various wing loadings.

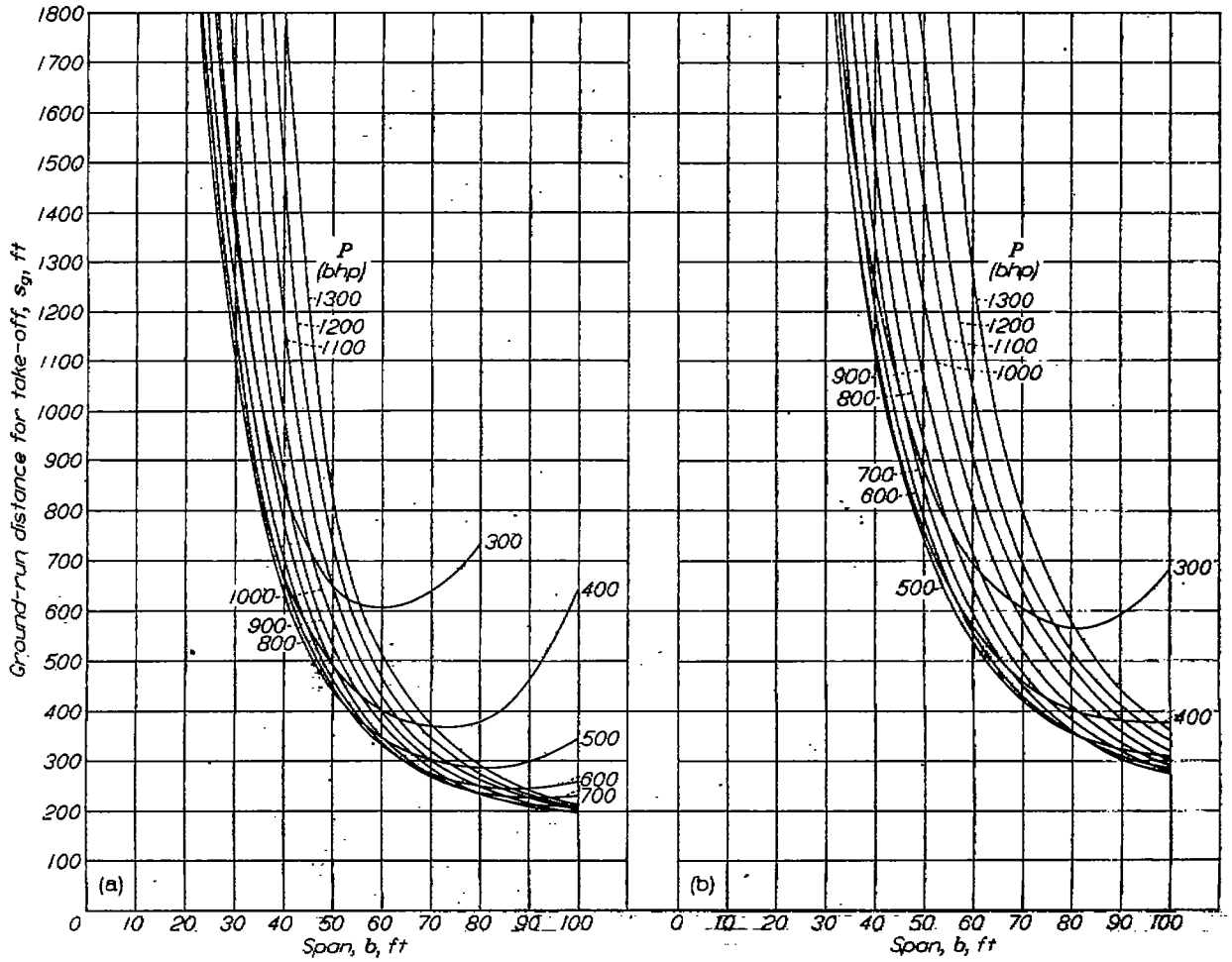

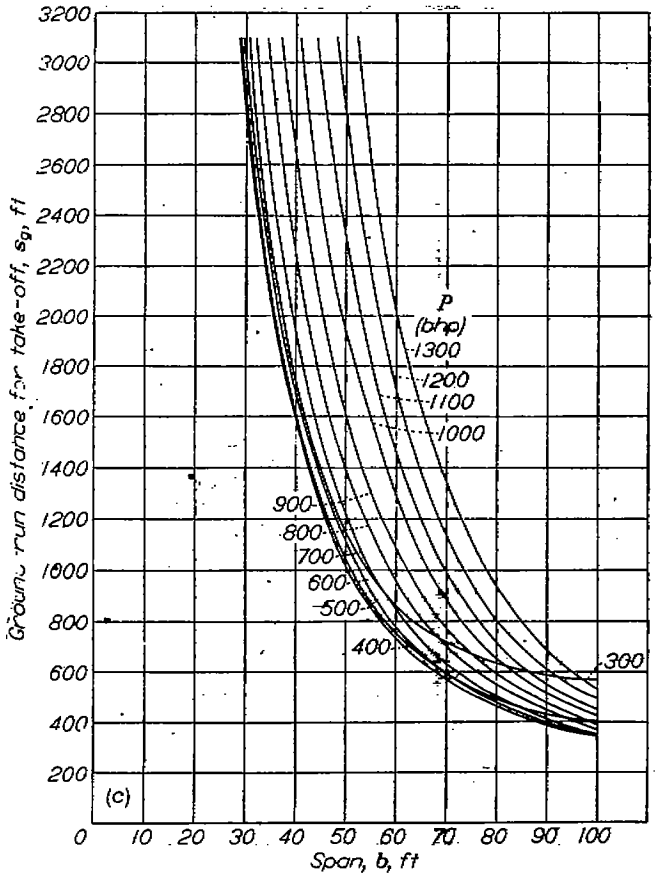

(a) $A=5$. (b) $A=10$. (c) $A=15$.

FIGURE 19.—Ground-run distance for take-off for an airplane without boundary-layer control as a function of span for various powers.

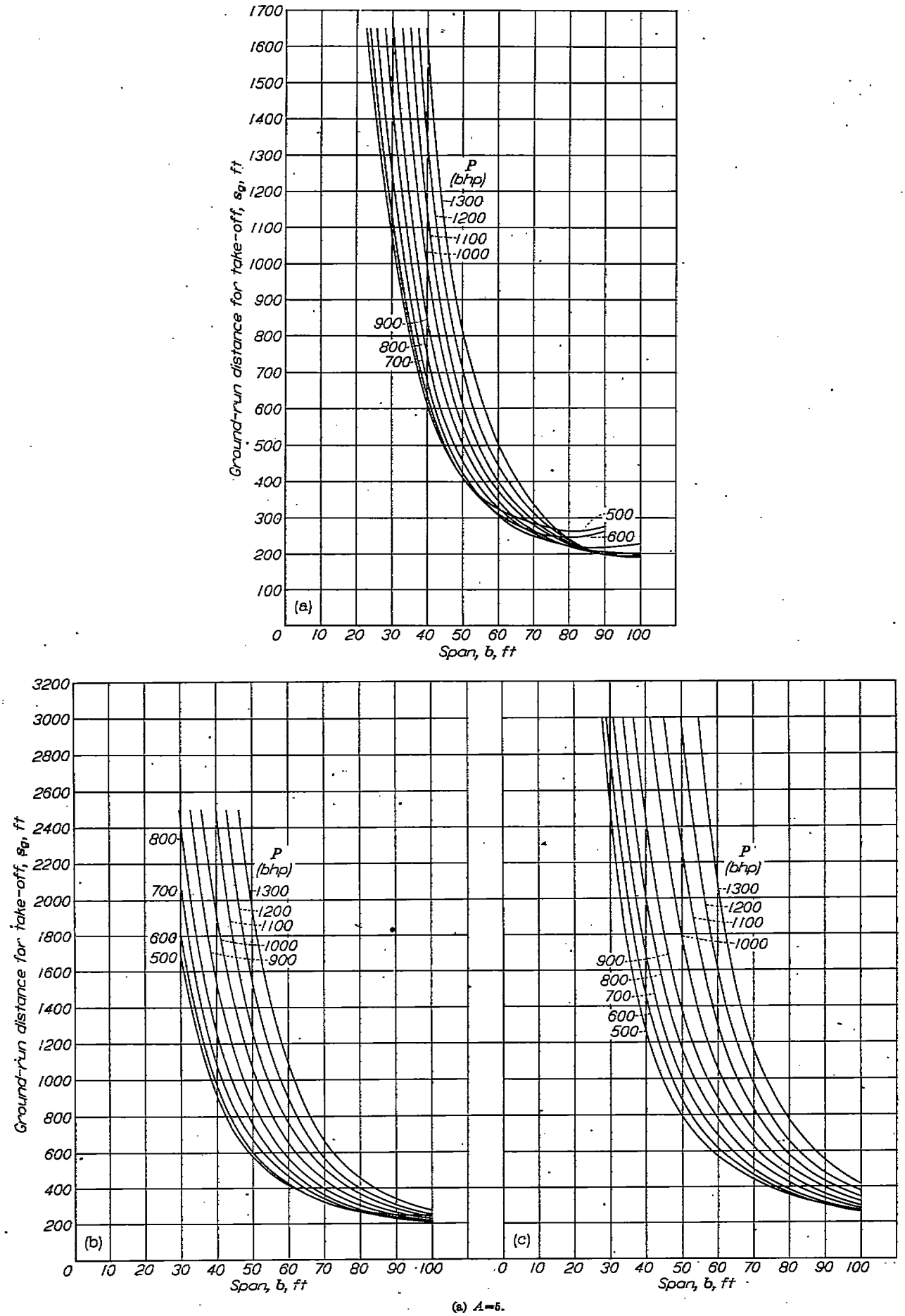

(a) A=5.

(b) A=10.

(c) A=15.

FIGURE 20.—Ground-run distance for take-off for an airplane with boundary-layer control as a function of span for various powers.

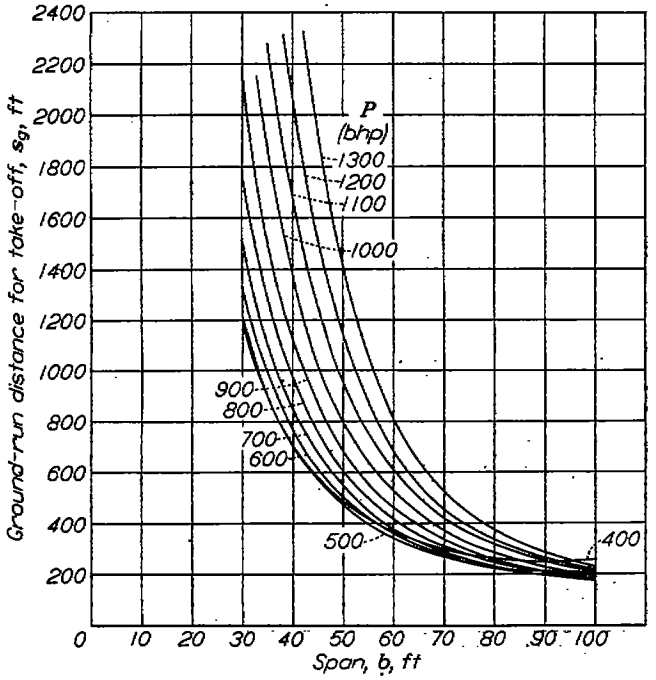

FIGURE 21.—Ground-run distance for take-off for an airplane with boundary-layer control, but with weight of boundary-layer equipment excluded, as a function of span for various powers. $A=10$.

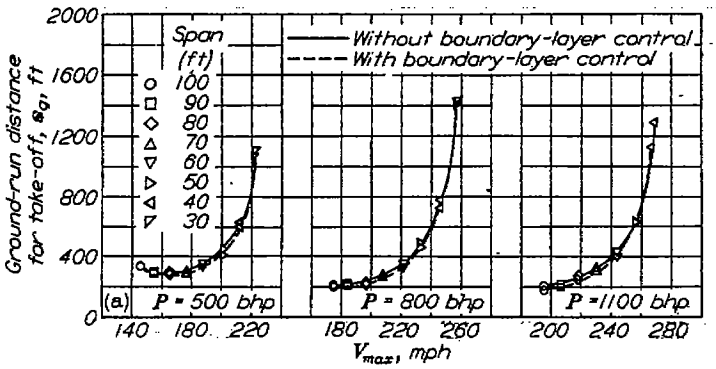

(a) $A=5$; $C_{L_{max}}=3.8$.

FIGURE 22.—Ground-run distance for take-off for an airplane with and without boundary-layer control as a function of maximum speed for various powers.

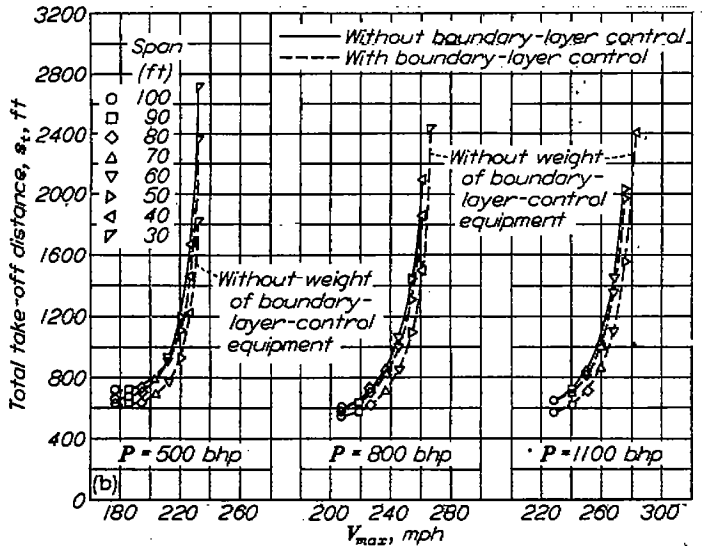

(b) $A=10$; $C_{L_{max}}=5.0$.

FIGURE 22.—Continued.

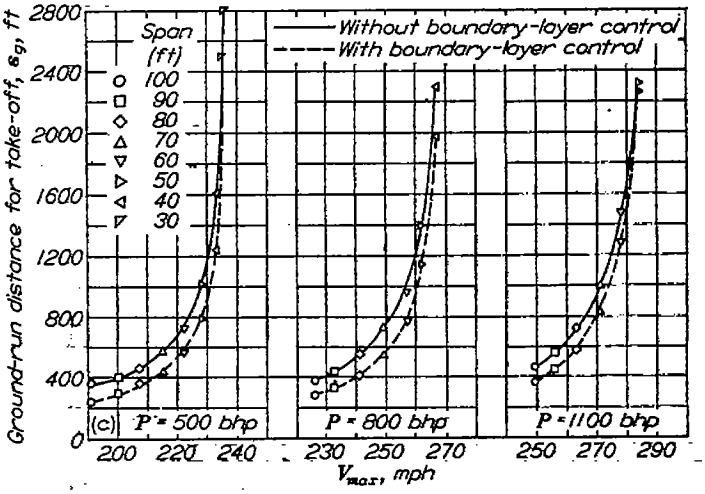

(c) $A=15$; $C_{L_{max}}=5.0$.

FIGURE 22.—Concluded.

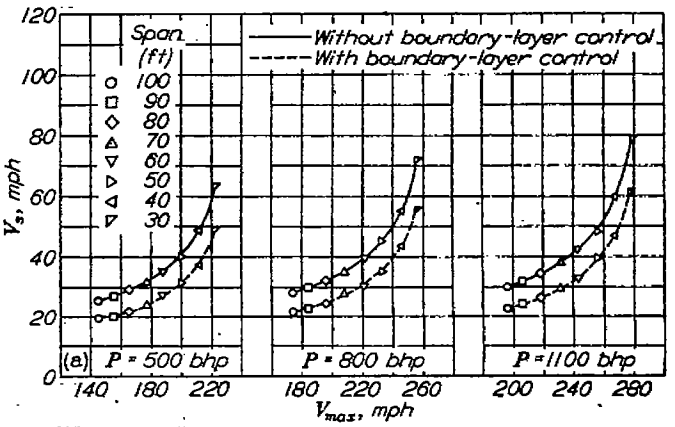

(a) $A=5$.

FIGURE 23.—Stalling speed of an airplane with and without boundary-layer control as a function of maximum speed for various powers.

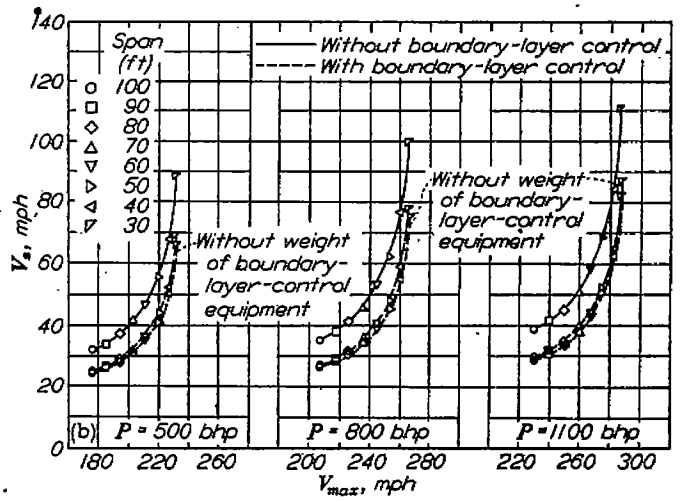

(b) $A=10$.

FIGURE 23.—Continued.

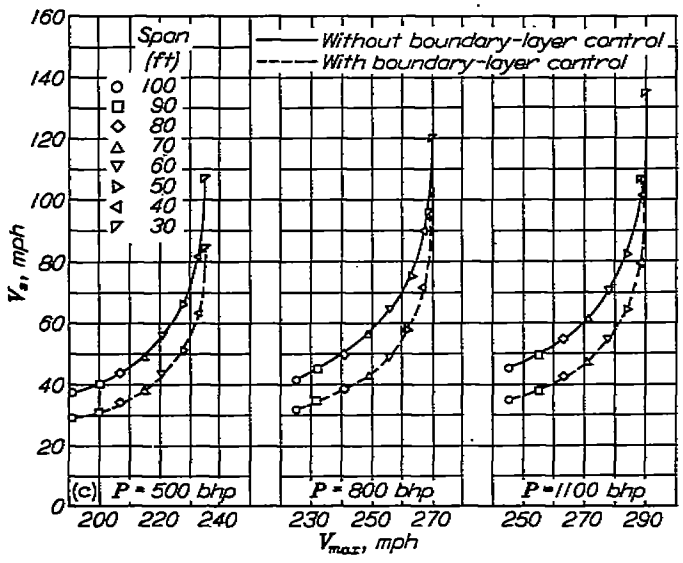

(c) A=15.

FIGURE 23.—Concluded.

POWER-OFF LANDING CHARACTERISTICS

The power-off landing characteristics to be discussed are

(1) The total landing distance

(2) The ground-run distance

(3) The speed at which the different phases of the landing maneuver are executed

Total landing distance.—The total landing distance is presented as a function of wing span in figure 24 with power as the parameter. The data are for aspect ratios of 5, 10, and 15 and are for the airplanes with and without boundary-layer control. An examination of the data of figure 24 indicates that, for a given engine power and aspect ratio, the landing distance decreases rapidly with increasing span over a certain range of spans, after which further increases in span have little effect. This is a result of the manner in which the wing loading varies with span. (See figs. 7 and 8.) For a given wing span, the landing distance is seen to increase with increasing engine power. In all cases, increasing the aspect ratio for a fixed span and power increases the total landing distance. For any given aspect ratio, the shortest landing distance is obtained for the airplane with largest span and lowest power. These trends are evident in the data for all configurations investigated. The effect of boundary-layer control on the total landing distance can best be seen in figure 25. In this figure the ratio of the total landing distance with boundary-layer control to the total distance without boundary-layer control is plotted as a function of span. The data clearly indicate that, regardless of engine power or aspect ratio, the use of maximum lift coefficients of the order of 5.0 which can be obtained with boundary-layer control as compared with lift coefficients of 2.8 which can be obtained without boundary-layer control results in decreases in the total landing distance which vary between 25 and 40 percent.

The data of figure 26 show that, for a constant wing loading, the use of boundary-layer control results in reductions of the total landing distance which vary from about 27 to 43 percent. The slightly more favorable effect of boundary-layer control when the comparison is based on a constant wing loading rather than on a constant span is explained by the fact that the addition of boundary-layer control to the airplane of constant span increases the wing loading by a small amount which has an adverse effect on the landing distance. For a constant wing loading, variations in the engine power have a negligible effect upon the landing distance (fig. 26); hence, the relatively large adverse effect of increasing the power upon the landing distance of an airplane of constant span, shown by the data of figure 24, results from the effect of engine power on wing loading. It might also be thought that the adverse effect upon the landing distance of increasing the aspect ratio for a given span and power (fig. 24) could be attributed entirely to an increase in wing loading. The data of figure 26, however, show that for a given wing loading, increasing the aspect ratio also causes some increase in the landing distance. This unfavorable effect of increasing aspect ratio on the landing distance results from the fact that as the aspect ratio is increased the airplane lift-drag ratio is also increased so that there results a flatter glide and, hence, a greater horizontal distance from the 50-foot obstacle to the point of ground contact. The proper application of a spoiler or air brake might, therefore, reduce or eliminate the unfavorable effect of increasing aspect ratio on the total landing distance.

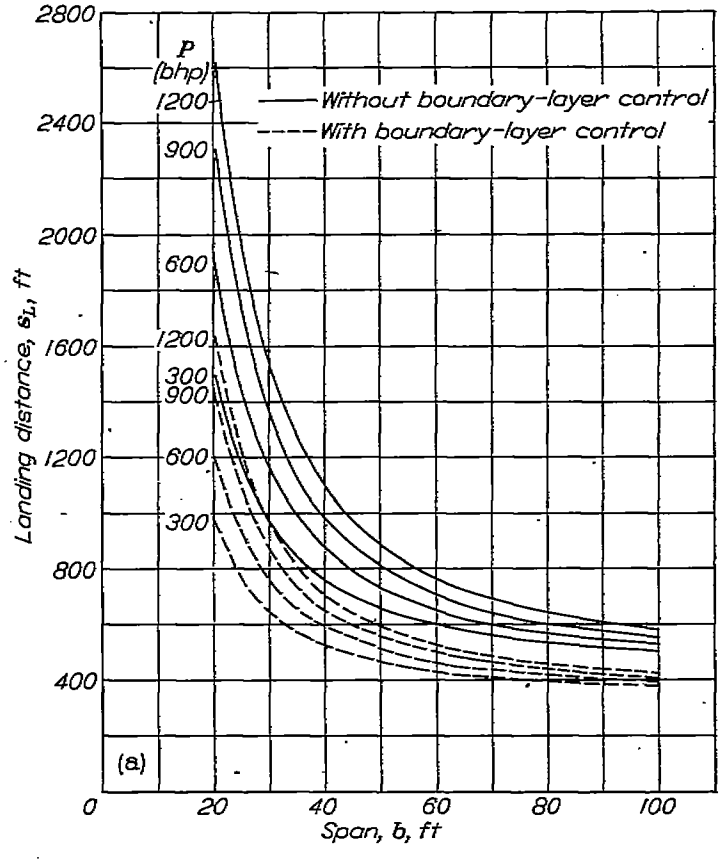

(a) A=5.

FIGURE 24.—Landing distance of an airplane with and without boundary-layer control as a function of span for various powers.

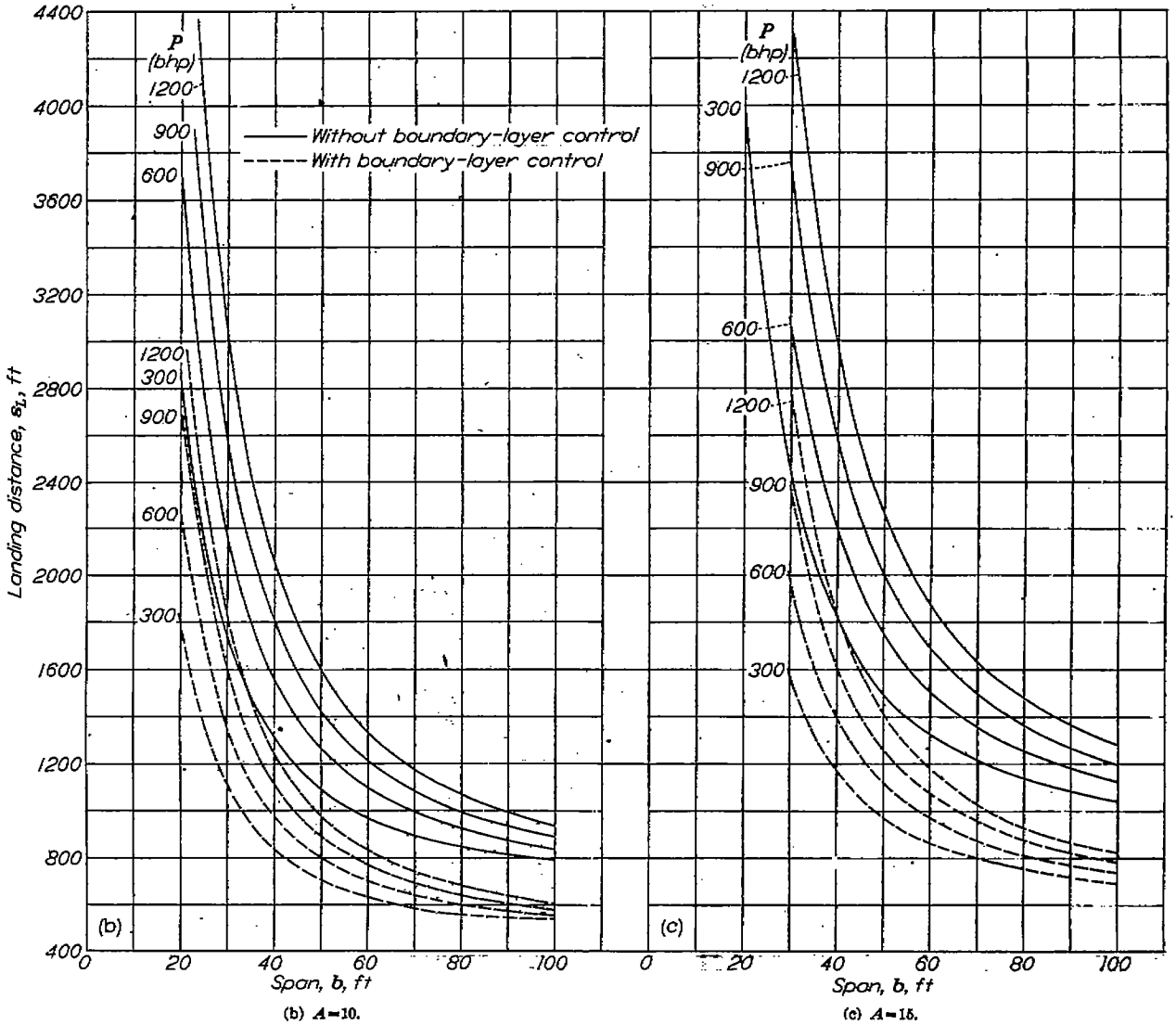

(b) $A=10$. (c) $A=15$.

FIGURE 24.—Concluded.

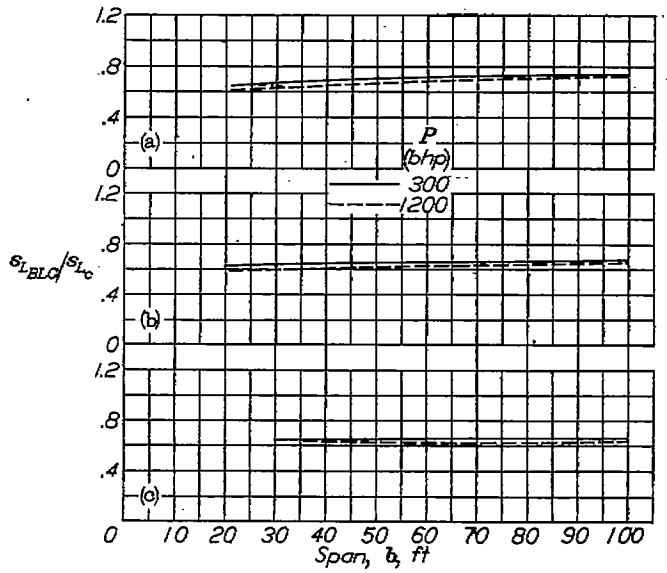

(a) $A=5$.
(b) $A=10$.
(c) $A=15$.

FIGURE 25.—Landing distance of airplane with boundary-layer control as a fraction of landing distance of same airplane without boundary-layer control.

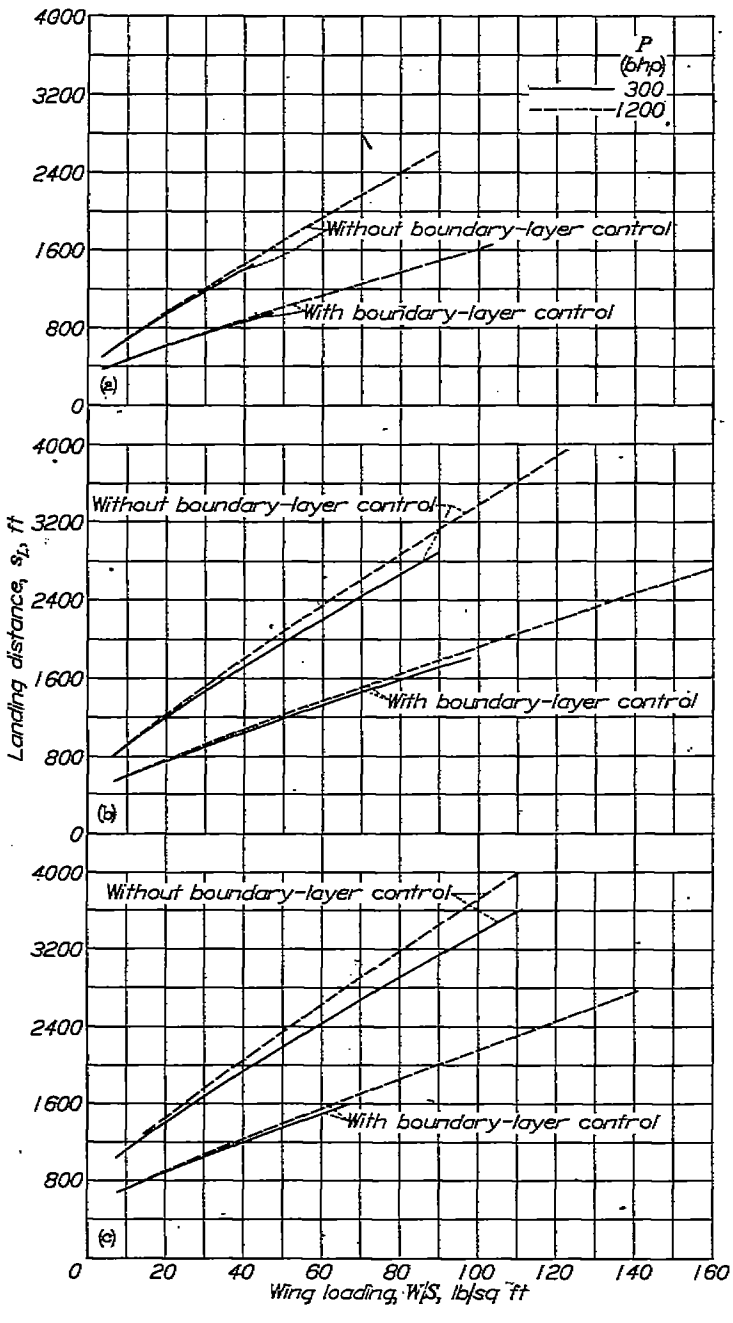

(a) A=5.
(b) A=10.
(c) A=15.

FIGURE 26.—Landing distance of an airplane with and without boundary-layer control as a function of wing loading.

The over-all conclusion to be drawn from the data of figures 24 to 26 is that boundary-layer control causes a substantial reduction in the total landing distance of all the airplane configurations investigated. The minimum landing distance for the configurations investigated was obtained for the airplane configuration having boundary-layer control and the lowest wing loading and aspect ratio—that is, a wing loading of 4 pounds per square foot and an aspect ratio of 5.

As previously pointed out, the application of boundary-layer control does not have any appreciable effect upon the maximum speed. Consequently, the reductions in landing distance resulting from boundary-layer control (figs. 24 to 26) can be obtained without any sacrifice in maximum speed in most cases. In order to show this effect more clearly, the total landing distance has been plotted against maximum speed in figure 27 for the airplanes with and without boundary-layer control. Figure 27 shows that for a given maximum speed the use of boundary-layer control results in a 25 to 40 percent decrease in the landing distance. The wing spans of the different airplanes are indicated by symbols on these curves. It is interesting to note that for most cases large increases in the maximum speed can be obtained with no increase in the landing distance by the use of boundary-layer control along with reduction in span. The unfavorable effect of increasing aspect ratio on the landing distance for a given maximum speed is, as previously pointed out, a result of the higher lift-drag ratio of the airplanes of high aspect ratio. The fact that boundary-layer control does not have a favorable effect upon the landing distance for the highest maximum speeds obtainable with a given power is explained by the data of figures 4 and 5 which show that the highest possible speed for a given power is slightly higher for the airplane without boundary-layer control than for the airplane with boundary-layer control. This is due to the increased wing loading of the boundary-layer-control airplane.

The data presented in figures 24 to 27 lead to the conclusion that the high lift coefficients available with boundary-layer control are very effective in reducing the landing distance of the type of airplane considered in this investigation. A somewhat different conclusion was reached with respect to the effect on the total take-off distance of the increased lift coefficients available with boundary-layer control. The data of figure 16 showed that there was no appreciable decrease in the total take-off distance due to boundary-layer control for a given maximum speed unless the aspect ratio was of the order of 15. Even for the higher aspect ratios, the relative effect of boundary-layer control on the total take-off distance is small as compared with its effect on the landing distance.

Ground-run distance.—The ground-run distance is plotted against wing span for different aspect ratios and engine horsepowers in figure 28 and against maximum speed in figure 29. The data of figure 28 indicate that the use of boundary-layer control results in reductions of the ground-run distance which vary from 30 to 40 percent depending upon the configuration. The use of the lowest possible wing loading—that is, low aspect ratio and engine of low power—gives the the shortest ground-run distance for a given span.

The data of figure 29 indicate that, for nearly all configurations, reductions in the ground-run distance of 35 to 40 percent can be obtained by the use of boundary-layer control without compromising the maximum speed. In comparison with the trends of figure 29, the data of figure 22 indicated that boundary-layer control has an important effect upon the ground run to take-off for a given maximum speed only if the aspect ratio is of the order of 10 to 15 and that the ground run for take-off is generally longer than that for landing.

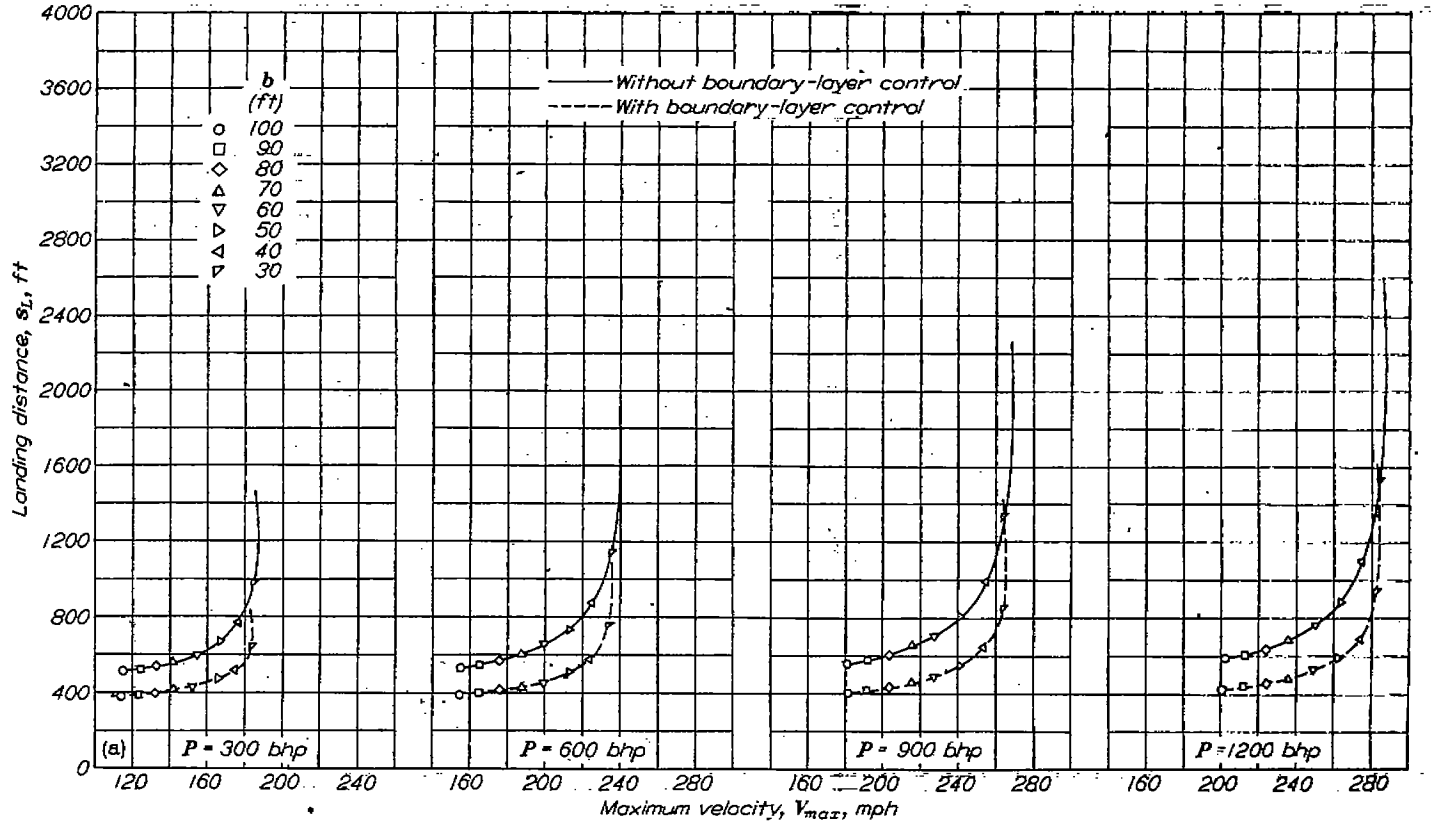

(a) $A=5$.

FIGURE 27.—Landing distance of an airplane with and without boundary-layer control as a function of velocity for various powers.

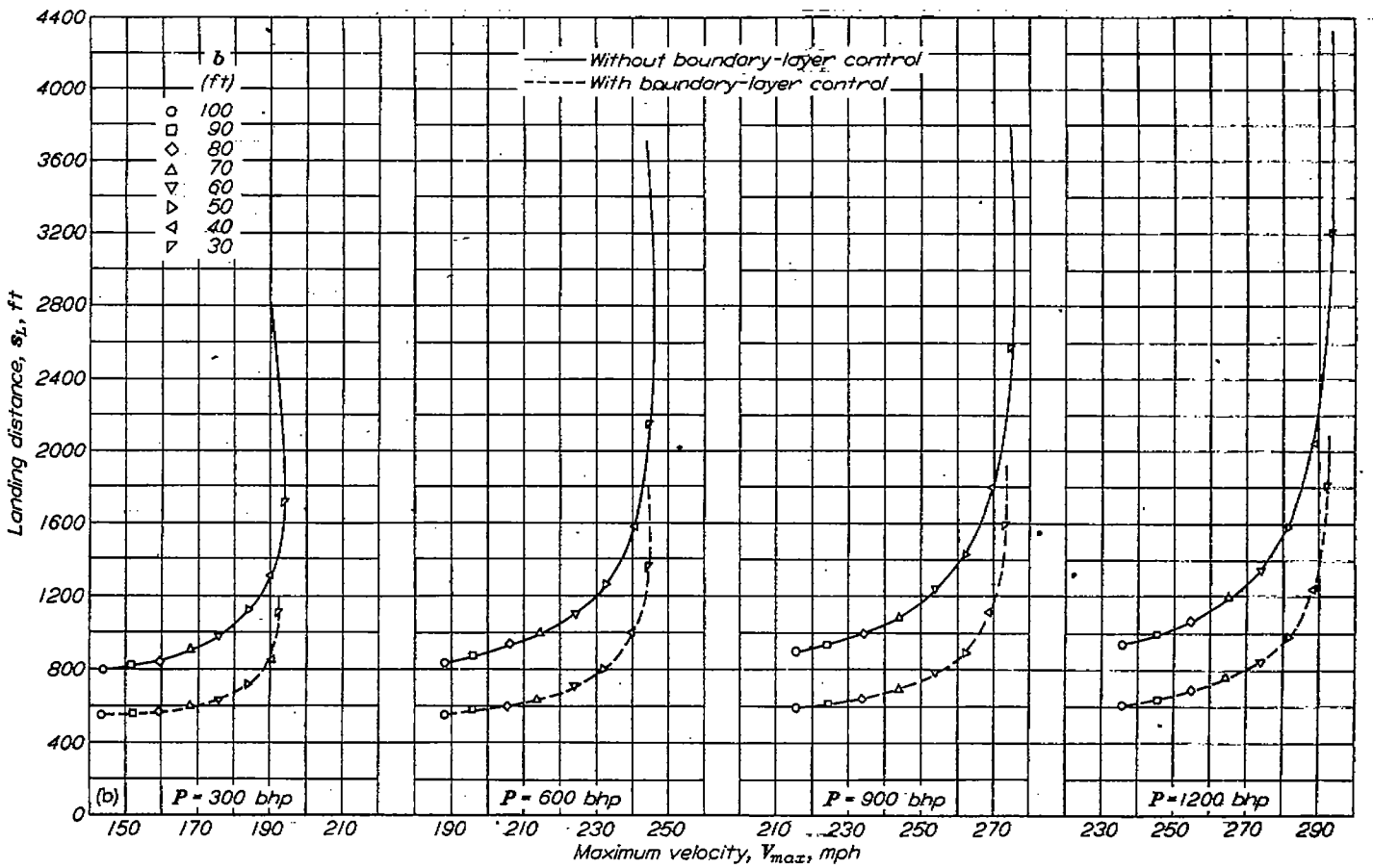

(b) $A=10$.

FIGURE 27.—Continued.

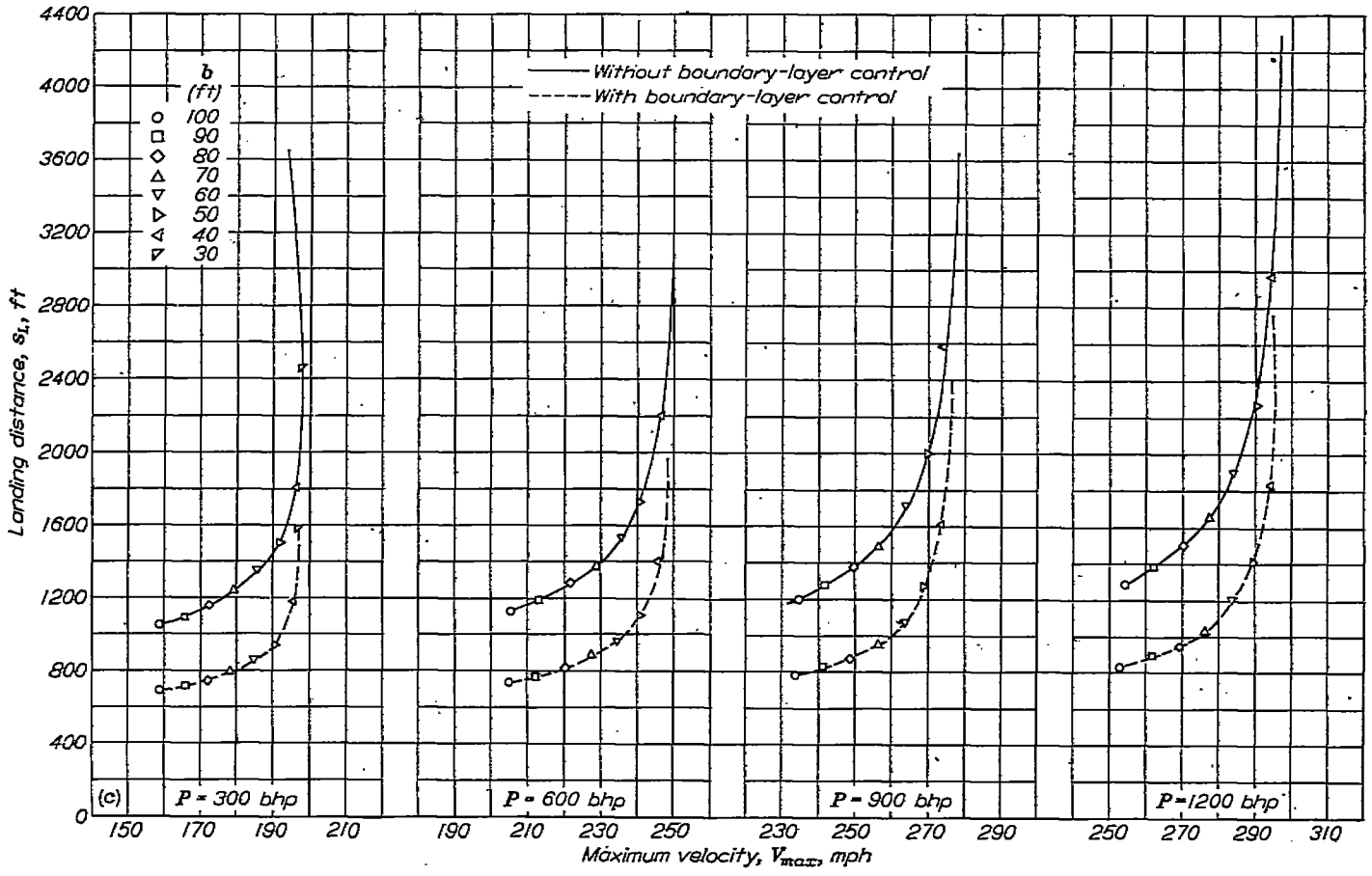

(c) $A=15$.

FIGURE 27.—Concluded.

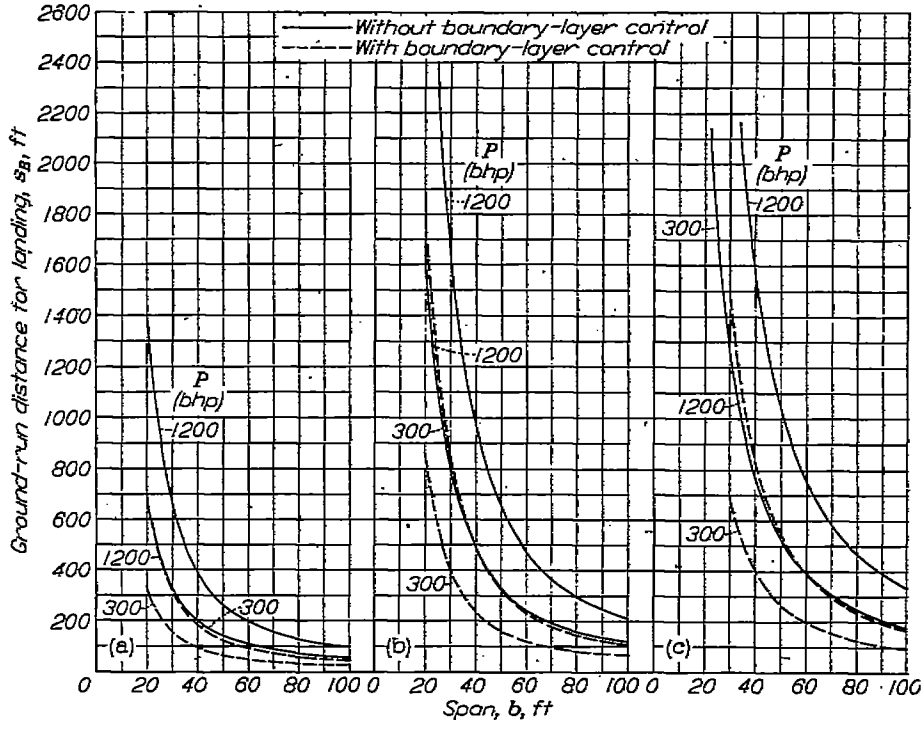

(a) $A=5$. (b) $A=10$. (c) $A=15$.

FIGURE 28.—Ground-run distance for landing for an airplane with and without boundary-layer control as a function of span.

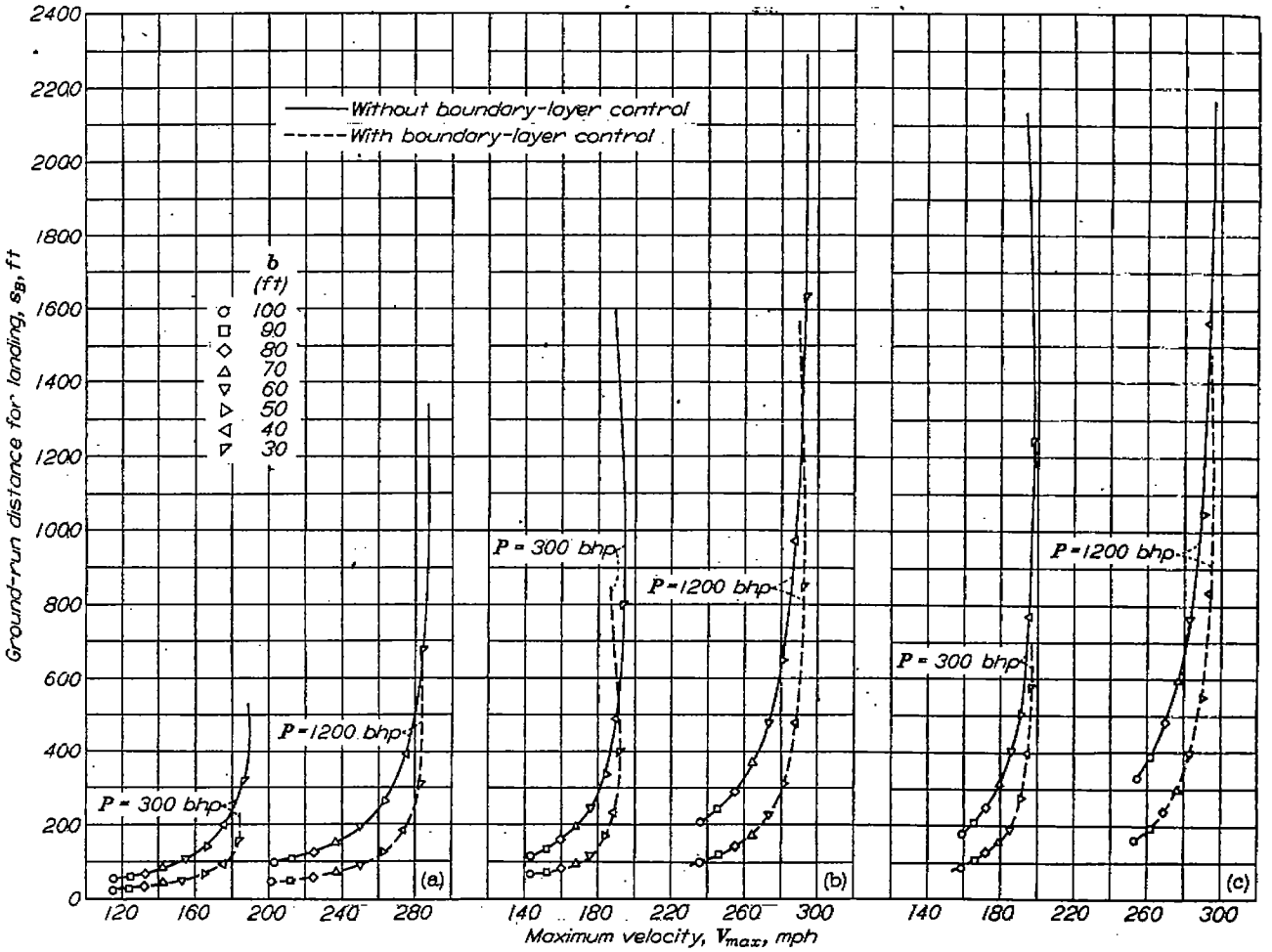

(a) $A=5$. (b) $A=10$. (c) $A=15$.

FIGURE 29.—Ground-run distance of an airplane with and without boundary-layer control as a function of maximum velocity.

Landing speeds.—The speeds with which the various phases of the landing maneuver are executed are of some importance as an indication of the piloting skill required to land a particular airplane. For this reason, data are given in figures 30 and 31 pertaining to the effect of boundary-layer control on the vertical or sinking speed in the steady glide and steady-glide speed.

The effect of boundary-layer control on the sinking speed is shown in figure 30 where the vertical velocity is plotted against wing span for various horsepowers and aspect ratios for the airplanes with and without boundary-layer control. The data show that boundary-layer control has only a relatively small effect on the sinking speed in all cases. For all the airplanes both with and without boundary-layer control, reducing the span for a given aspect ratio and engine power is seen to increase the sinking speed.

In figure 31 the velocity in the steady glide is plotted against wing span for the airplanes of different aspect ratio and power both with and without boundary-layer control. In all cases, the use of boundary-layer control is seen to reduce the speed in the steady glide by 20 to 25 percent. As would be expected, the steady-glide speed increases with decreasing span for a fixed power and aspect ratio in all cases. Increasing the aspect ratio for a given span and power also increases the gliding speed because of the associated increase in wing loading and wing lift-drag ratio.

EFFECT OF ASSUMPTIONS ON RESULTS

As was previously pointed out, most of the many assumptions employed in the analysis would not be expected to have any large effect on the landing and take-off performances of the boundary-layer-control airplane as compared with the airplane without boundary-layer control. Three assumptions were made, however, which should be considered in comparing the performance characteristics of the conventional and boundary-layer-control airplanes. These assumptions are

(1) No head wind

(2) No ground effect

(3) A ratio of span to root thickness of 35 and a thickness to chord ratio of 0.18 at the root and 0.12 at the tip

These three assumptions would probably have a greater effect on the boundary-layer-control airplane than on the conventional airplane for the following reasons.

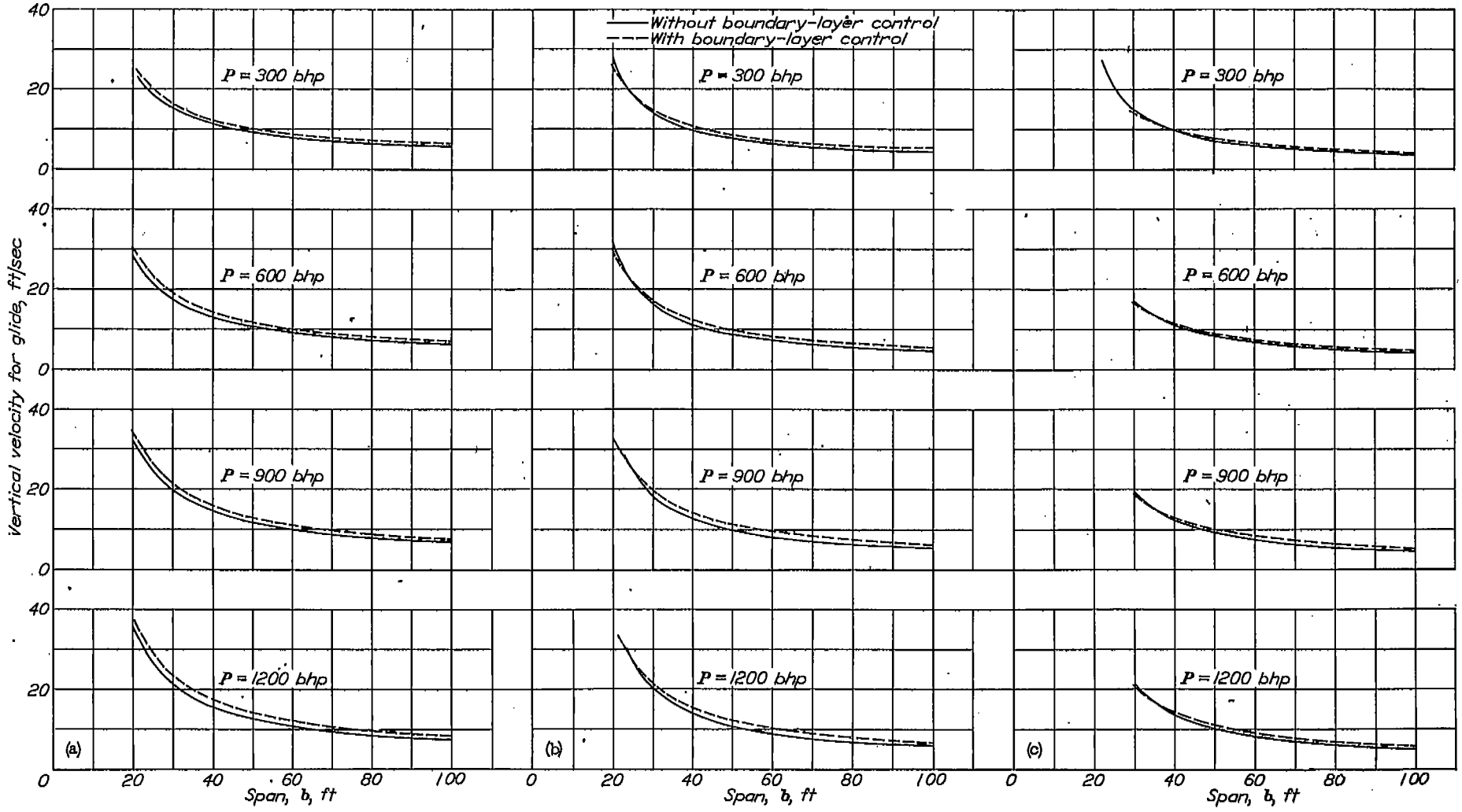

(a) $A=5$. (b) $A=10$. (c) $A=15$.

FIGURE 30.—Vertical velocity as a function of span for an airplane with and without boundary-layer control.

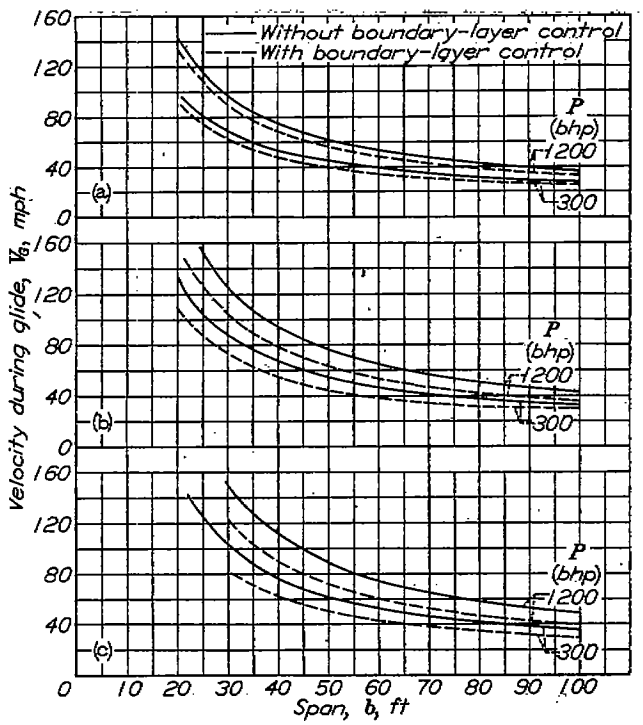

(a) $A=5$.
(b) $A=10$.
(c) $A=15$.

FIGURE 31.—Velocity during glide for an airplane with and without boundary-layer control as a function of span.

Head wind.—Because the maximum lift coefficients of the boundary-layer-control airplanes were greater than those of the conventional airplanes, the horizontal speed during the landing or take-off maneuver was less for the boundary-layer-control airplane than for the conventional airplane. Given a uniform head wind, the airspeeds of the two airplanes would remain unchanged, but the horizontal speed with respect to the ground of the slower airplane would be reduced by a greater percentage than that of the faster airplane. Therefore, the horizontal distance required to land from or take off and climb to a given altitude would be decreased in a head wind by a greater percentage for the boundary-layer-control airplane than for the conventional airplane.

Ground effect.—The effect of proximity to the ground is mainly that of increasing the effective aspect ratio. The greater aspect ratio would result in proportionately greater decreases in induced drag for the boundary-layer-control airplane with its high maximum lift coefficient than for the conventional airplane; therefore, the take-off distance for the boundary-layer-control airplane would be decreased by a greater percentage than that for the conventional airplane. For a more thorough treatment of this subject, see reference 16.

Wing thickness-chord ratios.—If the ratio of wing span to root thickness were maintained at 35, the root thickness-chord ratios of the wing would greatly exceed 0.18 for the larger spans and aspect ratios. The wing profile drag of the conventional airplane would, therefore, be considerably greater than the values used because of the large profile drags associated with airfoil sections having thickness ratios greater than 0.21 (reference 17). With boundary-layer control, however, it is possible to use the thicker airfoil sections without greatly increasing the profile drag as experimental results have indicated that, when separated flow exists, the drag of an airfoil section, including the boundary-layer-control power, may be less than the drag without boundary-layer control (references 2, 7, and 8).

CONCLUSIONS

An analysis was made to determine the effect of boundary-layer control on the take-off and power-off landing performance characteristics of a liaison type of airplane having aspect ratios ranging from 5 to 15, wing spans ranging from 25 to 100 feet, and engine brake horsepowers ranging from 300 to 1,300. The airplanes were assumed to have a 1,500-pound pay load and a cruising duration at 60-percent power of 5 hours. The results of the analysis indicate the following conclusions:

1. The addition of boundary-layer control does not reduce the absolute minimum total take-off distance which is obtained with a low wing loading and a moderately low aspect ratio.

2. The effectiveness of boundary-layer control in reducing the total take-off distance for a given maximum speed improves with increasing aspect ratio and, for wing loadings of 10 pounds per square foot or more and an aspect ratio of 10 or more, the addition of boundary-layer control results in a decrease in the total take-off distance of as much as 14 percent.

3. For a given maximum speed the ground-run distance for take-off was reduced for all configurations by the use of boundary-layer control. This reduction was negligible for an aspect ratio of 5 but was from 10 to 30 percent for aspect ratios of 10 and 15.

4. For a given maximum speed, the use of boundary-layer control resulted in a reduction in stalling speed of 20 to 25 percent for all configurations.

5. A reduction in the weight of the boundary-layer-control equipment would result in an appreciable decrease in the total take-off distance and ground-run distance for take-off, but its effect on the stalling speed would be negligible.

6. The optimum horsepower loading for minimum take-off distance was found to be approximately 8.5 and 9.0 pounds per horsepower for the conventional and boundary-layer-control airplanes, respectively.

7. For a specified airplane maximum speed, the total landing distance was reduced from 25 to 40 percent and the landing ground-run distance was reduced 30 to 40 percent by the use of boundary-layer control.

8. The gliding speeds were 20 to 25 percent lower for most of the airplanes with boundary-layer control than those for the airplanes without boundary-layer control.

9. For a fixed wing span, the sinking speed, or vertical velocity for the landing condition was slightly higher for the airplane with boundary-layer control than that for the conventional airplane.

LANGLEY AERONAUTICAL LABORATORY,
NATIONAL ADVISORY COMMITTEE FOR AERONAUTICS,
LANGLEY FIELD, VA., *October 4, 1951.*

REFERENCES

1. Hagerman, John R.: Wind-Tunnel Investigation of the Effect of Power and Flaps on the Static Lateral Stability and Control Characteristics of a Single-Engine High-Wing Airplane Model. NACA TN 1379, 1947.
2. Regenscheit, B.: Hochauftriebsversuche mit Absaugeklappenflügeln. Bericht A64 der LGL, 1938, pp. 27–34.
3. Stüper: Flight Experiences and Tests on Two Airplanes with Suction Slots. NACA TM 1232, 1950.
4. Ivey, H. Reese, Fitch, G. M., and Schultz, Wayne F.: Performance Selection Charts for Gliders and Twin-Engine Tow Planes. NACA MR L5E04, 1945.
5. Abbott, Ira H., Von Doenhoff, Albert E., and Stivers, Louis S., Jr.: Summary of Airfoil Data. NACA Rep. 824, 1945. (Formerly NACA ACR L5C05.)
6. Schrenk, Oskar: Experiments with a Wing from Which the Boundary Layer Is Removed by Suction. NACA TM 634, 1931.
7. Quinn, John H., Jr.: Tests of the NACA 65_3–018 Airfoil Section with Boundary-Layer Control by Suction. NACA CB L4H10, 1944.
8. Quinn, John H., Jr.: Wind-Tunnel Investigation of Boundary-Layer Control by Suction on the NACA 65_3–418, $a=1.0$ Airfoil Section with a 0.29-Airfoil-Chord Double Slotted Flap. NACA TN 1071, 1946.
9. Wood, Karl D.: Airplane Design. Fourth ed., Cornell Co-Op Soc., Ithaca, N. Y., June 1939.
10. Bridgman, Leonard, ed.: Janes's All the World's Aircraft. The Macmillan Co., 1942.
11. Krüger, W.: Calculations and Experimental Investigations on the Feed-Power Requirement of Airplanes with Boundary-Layer Control. NACA TM 1167, 1947.
12. Wetmore, J. W.: Calculated Effect of Various Types of Flap on Take-Off over Obstacles. NACA TN 568, 1936.
13. Hartman, Edwin P.: Considerations of the Take-Off Problem. NACA TN 557, 1936.
14. Gustafson, F. B.: Tire Friction Coefficients and Their Relation to Ground-Run Distance in Landing. NACA ARR, June 1942.
15. Diehl, Walter Stuart: Engineering Aerodynamics. The Ronald Press Co., rev. ed., 1936, p. 447.
16. Reid, Elliott G.: A Full-Scale Investigation of Ground Effect. NACA Rep. 265, 1927.
17. Neely, Robert H., Bollech, Thomas V., Westrick, Gertrude C., and Graham, Robert R.: Experimental and Calculated Characteristics of Several NACA 44-Series Wings with Aspect Ratios of 8, 10, and 12 and Taper Ratios of 2.5 and 3.5. NACA TN 1270, 1947.